# Chiral recognition at self-assembled multivalent (SAMul) nanoscale surfaces – enantioselectivity in polyanion binding

Ching W. Chan[a], Erik Laurini,[b] Paola Posocco,[b] Sabrina Pricl,[b] and David K. Smith*[,a]

a: Department of Chemistry, University of York, Heslington, York, YO10 5DD, UK
david.smith@york.ac.uk
b: Simulation Engineering (MOSE) Laboratory, Department of Engineering and Architectures (DEA), University of Trieste, Trieste, 34127, Italy

## SUPPORTING INFORMATION

### Contents

## 1. Materials and Methods

All reagents were obtained from commercial sources and used without further purification. Sodium salt heparin from porcine intestinal mucosa with a molecular weight between 15,000 ± 2,000 Da (1 KU = 1000 units) was obtained from Calbiochem®. Trizma® hydrochloride (Tris HCl) were obtained from Sigma Aldrich. Thin layer chromatography (TLC) was performed on Merck aluminium-backed plates, coated with 0.25 nm silica gel 60. $^{1}H$, $^{13}C$, $^{1}H$-$^{1}H$ COSY, $^{1}H$-$^{13}C$ HSQC and $^{1}H$-$^{13}C$ HMBC NMR were recorded on a JEOL ECX400 ($^{1}H$ 400 MHz, $^{13}C$ 100 MHz) spectrometer. ESI and HR-ESI mass spectra were recorded on a Bruker Daltonics MicroTOF mass spectrometer. IR spectra were measured on a PerkinElmer Spectrum Two™ IR Spectrometer with ATR-IR. Dynamic light scattering data were measured at 1 mg/mL using a Zetasizer Nano (Malvern Instruments Ltd., Worcestershire, UK), based on the principle of measurement of the backscattered light fluctuations at an angle of 173° and the calculation of an autocorrelation function. Data were recorded from 15–20 runs per single measurement, each of which was carried out at 25°C using folded capillary cells (DTS 1060). Monomer solutions were freshly prepared by dissolving an appropriate amount of dry compound in filtered aqueous media (e.g. 10 mM Tris HCl, 150 mM NaCl). All samples were agitated and incubated at 25°C for 10 minutes prior to measurement. Data are reported based on volume distribution. Circular Dichroism was carried out on a Jasco J810 CD Spectrophotometer (150W Xe lamp). Fluorescence emission was measured on a Hitachi F-4500 spectrofluorimeter. All MalB solutions were incubated at 50$^{o}$C for 24 hours prior to use and stored in the dark. For the purpose of calculations, the molecular weight of heparin is assumed as that of the sodiated analogue of a typical heparin repeat unit (L-iduronic acid and β-D-glucuronic acid), namely 665.40 g mol$^{-1}$.

## 2. Synthesis and Characterisation Data

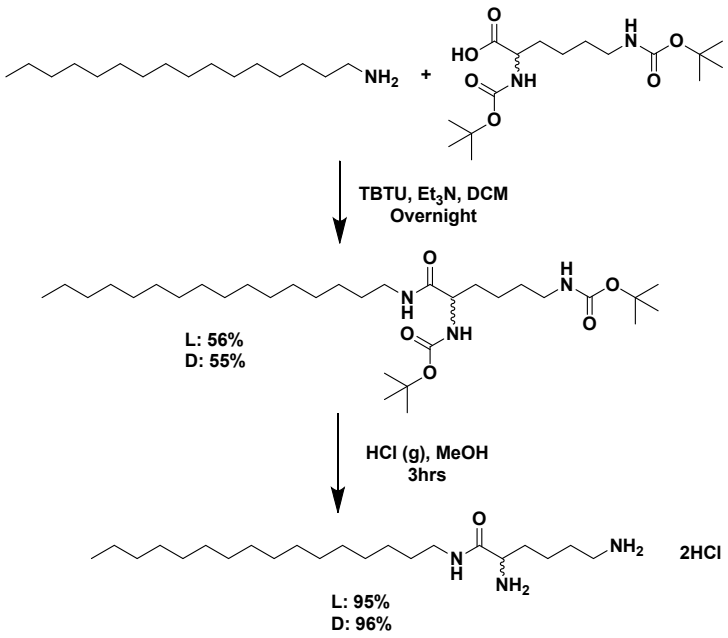


Scheme S1. Synthesis of $C_{16}$-L-Lys and $C_{16}$-D-Lys.

**Synthesis of $C_{16}$-L-Lys-$(Boc)_2$**

L-Lys-$(Boc)_2$ (500 mg, 1.44 mmol) was dissolved in DCM (40 ml) and TBTU (463 mg, 1.44 mmol) and $NEt_3$ (5 ml) were added. The mixture was stirred for 5 minutes, then 1-hexadecylamine (390 mg, 1.44 mmol) was dissolved in DCM (20 ml) and added to the mixture. The solution was left stirring overnight then the solvent was evaporated *in vacuo.* After evaporation of the solvent the product was dissolved again in EtOAc (50 ml) and washed with $NaHSO_4$ (1.33 M, 2x 15 ml), sat. $NaHCO_3$ (2x 15 ml), $H_2O$ (3x 15 ml) and sat. NaCl solution (15 ml). After column chromatography ($SiO_2$, Hexane:EtOAc 1:1), pure product was obtained as a pale yellow solid (0.466, 0.81 mmol 56%). $R_f$ = 0.25 (Hexane : EtOAc 1:1). $^1$H NMR (400 MHz, $CDCl_3$) δ: 6.72 (s, CHN*H*, 1H), 5.45 (s, $CH_2$N*H*, 1H), 4.82 (s, $CH_2$N*H*, 1H), 4.01 (dd app. q, *J* = 4.4 Hz, C*H*(NHBoc), 1H), 3.20-3.04 (m, CH(NHBoc)C$H_2$, 2H); 1.69, 1.52 (comp m, C$H_2$C$H_2$C$H_2$NHBoc, 4H), 1.34 (br s, C$(CH_3)_3$ + $CH_2$, 22H), 1.15 (br s, $CH_2$, 28H), 0.78 (t, *J* = 6.5 Hz, $CH_3$, 3H). $^{13}$C NMR (100MHz, $CDCl_3$) δ: 172.18 (C=O); 156.16, 155.88, (C=O, Boc); 79.65, 78.91, (*C*$(CH_3)_3$); 54.33 (*C*HCONH); 39.99 (*C*$H_2$NHBoc), 39.46 (CONH*C*$H_2$); 32.31, 31.90, 29.69, 29.66, 29.61, 29.57, 29.52, 29.35, 29.32 ($CH_2$); 28.43, 28.33, C(*C*$H_3)_3$; 26.92 22.73, 22.67 ($CH_2$); 14.10

($CH_3$) IR $cm^{-1}$: 3341*m* (N-H), 2918*m*, 2850*m* (C-H), 1685*s* (C=O), 1648*m*, 1532*s* (CONH), 1244*m*, 1166*s*, 655*m*. ESI-MS: Calcd. $[M+H]^+$ ($C_{32}H_{64}N_3O_5$) *m/z* = 570.4840; Obs. $[M+H]^+$*m/z*= 570.4868(100%).

**Synthesis of $C_{16}$-D-Lys-$(Boc)_2$**

The synthesis of this compound was as described for $C_{16}$-L-Lys-$(Boc)_2$ only using D-Lys-$(Boc)_2$ instead of L-Lys-$(Boc)_2$. The product was obtained as a pale yellow solid (0.452 g, 0.79 mmol, 55%). The characterisation data were equivalent to $C_{16}$-L-Lys-$(Boc)_2$.

**Synthesis of $C_{16}$-L-Lys**

$C_{16}$-L-Lys-$(Boc)_2$ (100 mg, 175 µmol) was dissolved in MeOH (20 ml) and HCl gas was bubbled through the solution for 20 s. The reaction mixture was stirred at room temperature for 3 h. The solvent was removed *in vacuo* to afford the product as an off-white foam (73 mg, 166 µmol, 95%). $R_f$ = 0.00 ($NH_4OH$). $^1$H NMR (400 MHz, MeOD-$d_4$) δ: 3.88 (dd app t, *J* = 4.4. Hz, C*H*($NH_2$), 1H), 3.21 (t, *J* = 7.0 Hz, C$H_2$NHCO, 2H); 2.94 (t, *J* = 8.0 Hz, C$H_2NH_2$, 2H) 1.88, 1.72 1.50 (comp m, C$H_2$C$H_2$C$H_2$C$H_2NH_2$, 6H), 1.28-1.26 (m, $CH_2$, 28H), 0.88 (t, *J* = 6.5 Hz, $CH_3$, 3H). $^{13}$C NMR (100MHz, MeOD-$D_4$) δ: 169.82 (C=O); 54.16 (*C*HCONH); 40.66 (*C*$H_2NH_2$,); 40.26 ($CH_2$NH); 33.06, 32.13, 30.79, 30.76, 30.71, 30.47, 30.40, 30.27, 28.80, 28.71, 28.04, 27.99, 23.73, 23.00 ($CH_2$); 14.48 ($CH_3$). IR $cm^{-1}$: 2916*m*, 2848*m* (C-H), 1667*m* (C=O), 1566*s* (CONH), 1269*w*, 720*m*. ESI-MS: Calcd. $[M+H]^+$ ($C_{22}H_{48}N_3O$) *m/z* = 370.3792; Obs. $[M+H]^+$ *m/z*=370.3772.

**Synthesis of $C_{16}$-D-Lys**

The synthesis of this compound was as described for $C_{16}$-L-Lys-$(Boc)_2$ only using $C_{16}$-D-Lys-$(Boc)_2$ instead of $C_{16}$-L-Lys-$(Boc)_2$. The product was obtained as pale yellow solid (74 mg, 167 µmol, 96%). The characterisation data were equivalent to $C_{16}$-L-Lys apart from CD spectroscopy (see Section 4).

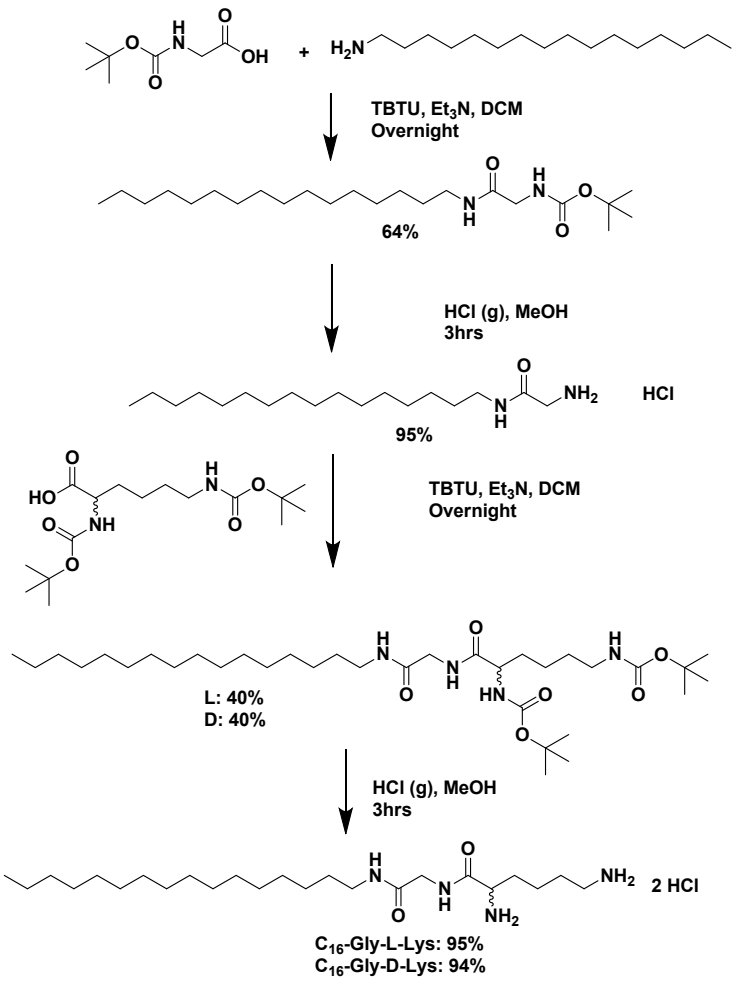


Scheme S2. Synthesis of $C_{16}$-Gly-L-Lys and $C_{16}$-Gly-D-Lys.

**Synthesis of $C_{16}$-Gly-Boc**

Boc-Gly-OH (1.48 g, 8.42 mmol) was dissolved in DCM (40 ml) and TBTU (463 mg, 8.32 mmol) and $NEt_3$ (5 ml) were added. The mixture was stirred for 5 min, then 1-hexadecylamine (2.00 g, 8.42 mmol) was dissolved in DCM (20 ml) and added to the mixture. The solution was left stirring overnight then the solvent was evaporated *in vacuo.* After evaporation of the solvent the product was dissolved again in EtOAc (50 ml) and washed with $NaHSO_4$ (1.33 M, 2x 15 ml), sat. $NaHCO_3$ (2x 15 ml), $H_2O$ (3x 15 ml) and sat. NaCl solution (15 ml). The solvent was evaporated *in vacuo* and the product was obtained as a white solid (1.3 g, 5.39 mmol, 64%). $R_f$ = 0.40 (Hexane:EtOAc 1:1). $^1$H NMR (400 MHz, $CDCl_3$) δ: 6.11 (br s, NH, 1H); 5.15 (br s, NH, 1H); 3.76 (d, *J* = 4.4 Hz, COC*H*$_2$NH, 2H); 3.25 (q, *J* = 4.4 Hz, C*H*$_2$NHCO, 2H) 1.67, 1.50-1.28 (comp m, C($CH_3$)$_3$ + $CH_2$, 37H), 0.86 (t, $CH_3$, *J* = 8.0 Hz, 3H). $^{13}$C NMR (100MHz, $CDCl_3$) δ: 169.34, 156.47 (C=O); 80.45 *C*($CH_3$)$_3$; 39.59 (CO*C*H$_2$NH); 32.01 (*C*H$_2$NHCO); 29.78, 29.75, 29.68, 29.62,

29.60, 29.45, 29.37 ($CH_2$); 28.38 ($C(CH_3)_3$); 26.94, 22.7 ($CH_2$); 14.22 ($CH_3$). IR $cm^{-1}$: 3287*m* (N-H), 2916*m*, 2848*m* (C-H), 1693*s* (C=O), 1642*s*, 1530*m* (CONH), 1249*m*, 1170*s*, 719*m*. ESI-MS: Calcd. $[M+Na]^+$ ($C_{23}H_{46}N_2O_3Na$) *m/z* = 421.3401; Obs. $[M+H]^+$ *m/z* = 421.3390 (100%)

**Synthesis of $C_{16}$-Gly**

$C_{16}$-Gly-Boc (600 mg, 1.51 mmol) was dissolved in MeOH (20 ml) and HCl gas was bubbled through the solution for 20 s. The reaction mixture was stirred at room temperature for 3 h. The solvent was removed *in vacuo* to afford the product as an off-white foam (481 mg, 1.43 mmol, 96%). $R_f$ = 0.00 ($NH_4OH$). $^1H$ NMR (400 MHz, MeOD- $d_4$) δ: 3.65, (s, $CH_2NH_2$, 2H); 3.28 (t, *J* = 8.0 Hz, $CH_2NHCO$, 2H) 1.49 (app. q, *J* = 8.0 Hz, $CH_2CH_2NHCO$ 2H); 1.35-1.20 (comp m, $CH_2$, 26H), 0.90 (t, *J* = 7.0 Hz, $CH_3$, 3H). $^{13}C$ NMR (100MHz, MeOD-$d_4$) δ: 165.68 (C=O); 40.66 ($CH_2NH_2$); 40.26 ($CH_2NHCO$); 31.75, 29.45, 29.37, 29.02, 26.65 22.41 ($CH_2$); 13.11. ($CH_3$). IR $cm^{-1}$: 3287*m* (N-H), 2914*m*, 2848*m* (C-H), 1642*s* (C=O), 1470*s* (CONH), 1114*w*, 661*m*. ESI-MS: Calcd. $[M+H]^+$ ($C_{18}H_{39}N_2O$) *m/z* = 299.3057; Obs. $[M+H]^+$ *m/z* = 299.3068 (60%), ($C_{18}H_{38}N_2NaO$) *m/z* = 321.2876; Obs. $[M+H]^+$ *m/z* = 321.2883 (40%).

**Synthesis of $C_{16}$-Gly-L-Lys-Boc**

L-Lys-$(Boc)_2$ (283 mg, 0.60 mmol) was dissolved in DCM (40 ml) and TBTU (191.7 mg, 1.44 mmol) and $NEt_3$ (5 ml) were added. The mixture was stirred for 5 min, then $C_{16}$-Gly (200 mg, 0.60 mmol) was dissolved in DCM (20 ml) and added to the mixture. The solution was left stirring overnight then the solvent was evaporated *in vacuo.* After evaporation of the solvent the product was dissolved again in EtOAc (50 ml) and washed with $NaHSO_4$ (1.33 M, 2x 15 ml), sat. $NaHCO_3$ (2x 15 ml), $H_2O$ (3x 15 ml) and sat. NaCl solution (15 ml). The solvent was evaporated *in vacuo* and the product was obtained as pale yellow solid (150 mg, 0.24 mmol, 40%). $R_f$ = 0.30 (Hexane:EtOAc 1:1). $^1H$ NMR (400 MHz, $CDCl_3$) δ: 7.49 (s, NH, 1H), 7.09 (s, NH, 1H), 5.85 (s, NH, 1H), 5.27 (s, NH, 1H), 4.12 (dd app q, *J* = 4.4 Hz, C*H*(NHBoc), 1H), 3.81 (s, $NHCH_2CONH$, 2H) 3.20-3.04 (m, $CH_2NH$, 4H); 1.69-1.52 (comp m, $CH_2CH_2CH_2NHBoc$, 4H), 1.35-1.33 (m, $C(CH_3)_3$ + $CH_2$, 22H), 1.16-1.14 (m, $CH_2$, 26H), 0.77 (t, *J* = 7.0 Hz, $CH_3$, 3H). $^{13}C$ NMR (100MHz, $CDCl_3$) δ: 173.31, 169.08 (C=O); 156.45, 156.34 (CONHBoc) 79.98, 78.99, ($C(CH_3)_3$); 55.32 (CO*C*HNH); 43.07 ($CH_2NHBoc$,), 39.68 ($NHCH_2CO$) 31.39, 29.70, 29.69,

29.66, 29.59, 29.55, 29.42, 29.36 ($CH_2$); 29.36, 28.47 ($C(CH_3)$); 26.98, 22.68 ($CH_2$) 14.13 ($CH_3$). IR $cm^{-1}$: 3301*m* (N-H), 2922*m*, 2852*m* (C-H), 1692*s* (C=O), 1649*m* (C=O), 1525*s* (CONH), 1248*m*, 1168*s*, 719*m*. ESI-MS: Calcd. $[M+Na]^+$ ($C_{36}H_{66}N_4NaO_6$) *m/z* = 649.4875; Obs. $[M+H]^+$ *m/z* = 649.4862 (100%)

**Synthesis of $C_{16}$-Gly-D-Lys-Boc**

The synthesis of this compound was as described for $C_{16}$-L-Lys-$(Boc)_2$ only using D-Lys-$(Boc)_2$ instead of L-Lys-$(Boc)_2$. The product was obtained as a pale yellow solid in (150 mg, 0.24 mmol, 40%). The characterisation data were equivalent to $C_{16}$-Gly-L-Lys-$(Boc)_2$.

**Synthesis of $C_{16}$-Gly-L-Lys**

$C_{16}$-Gly-L-Lys-$(Boc)_2$ (100 mg, 159 µmol) was dissolved in MeOH (20 ml) and HCl gas was bubbled through the solution for 20 s. The reaction mixture was stirred at room temperature for 3 h. The solvent was removed *in vacuo* to afford the product as an off-white foam (75 mg, 151 µmol, 95%). $R_f$ = 0.00 ($NH_4OH$). $^1$H NMR (400 MHz, MeOD-$d_4$) δ:, 4.12 (t, C$H_2$NH, *J* = 4.4 Hz, 2H), 3.81 (s, NHC$H_2$CONH, 2H) 3.20 (m, C$H_2$NHCO, 2H); 2.96 (t, CONHC$H_2$, *J* = 7.5 Hz, 2H); 1.92, (m, $NHCOCH_2CH_2$, 2H) 1.69, 1.52 (m, $CH_2CH_2CH_2NH_2$ + $CH_2$, 6H), 1.35-1.33 (m, $C(CH_3)_3$ + $CH_2$, 26H), 0.77 (t, *J* = 7.0 Hz, $CH_3$, 3H). $^{13}$C NMR (100MHz, MeOD-$d_4$) δ: 169.51, 169.22 (C=O); 52.90 (*C*HCONH); 41.77 ($CH_2NH_2$); 39.29 (CONH$CH_2$); 31.75, 30.45, 29.47, 29.44, 29.40, 29.16, 29.06, 26.71, 26.63, 22.42, 21.31 ($CH_2$); 13.15. ($CH_3$). IR $cm^{-1}$: 3229*m* (N-H), 291*m*, 2849*m* (C-H), 1654*m* (C=O) 1562*s* (CONH), 1251*m*, 720*m*. ESI-MS: Calcd. $[M+H]^+$ ($C_{24}H_{51}N_4O_2$) *m/z* = 427.4007; Obs. $[M+H]^+$ *m/z* = 427.3987, 100%.

**Synthesis of $C_{16}$-Gly-D-Lys**

The synthesis of this compound was as described for $C_{16}$-Gly-L-Lys-$(Boc)_2$ only using $C_{16}$-Gly-D-Lys-$(Boc)_2$ instead of $C_{16}$-Gly-L-Lys-$(Boc)_2$. The product was obtained as an off-white foam (74 mg, 167 µmol, 94%). The characterisation data were equivalent to $C_{16}$-Gly-L-Lys apart from CD spectroscopy (see Section 4).

## 3. Dynamic Light Scattering Data

In cases where the quality report is flagged, this is a result of sample polydisperisity making cumulant fit error high – this means that the 'averaged' results for the whole trace presented in red should be disregarded – the results listed for the individual peaks are still valid.

**$C_{16}$-L-Lys**

| | | | Size (d.nm): | % Volume: | St Dev (d.nm): |
|---|---|---|---|---|---|
| Z-Average (d.nm): | 15.38 | Peak 1: | 6.167 | 100.0 | 1.716 |
| PdI: | 0.616 | Peak 2: | 115.0 | 0.0 | 47.63 |
| Intercept: | 0.897 | Peak 3: | 0.000 | 0.0 | 0.000 |

Result quality : Refer to quality report

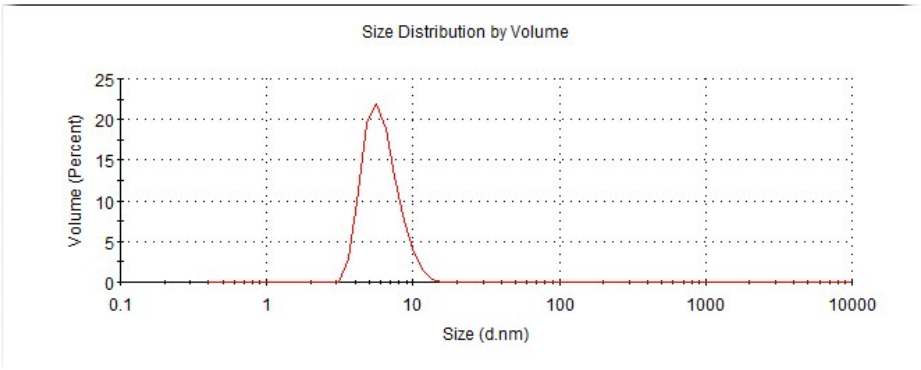


Fig. S1. DLS data for $C_{16}$-L-Lys measured at 1 mg/mL.

**$C_{16}$-D-Lys**

| | | | Size (d.nm): | % Volume: | St Dev (d.nm): |
|---|---|---|---|---|---|
| Z-Average (d.nm): | 65.02 | Peak 1: | 6.270 | 100.0 | 1.697 |
| PdI: | 0.181 | Peak 2: | 124.0 | 0.0 | 43.52 |
| Intercept: | 0.887 | Peak 3: | 0.000 | 0.0 | 0.000 |

Result quality : Refer to quality report

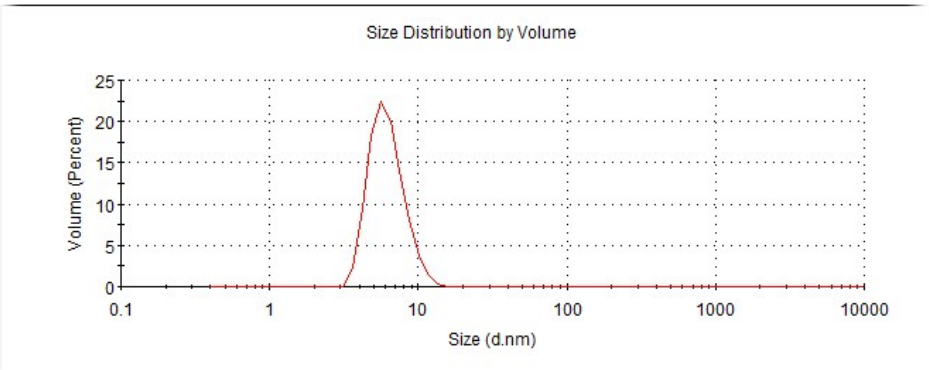


Fig. S2. DLS data for $C_{16}$-D-Lys measured at 1 mg/mL.

**$C_{16}$-Gly-L-Lys**

| | | | Size (d.nm): | % Volume: | St Dev (d.nm): |
|---|---|---|---|---|---|
| Z-Average (d.nm): | 117.8 | Peak 1: | 119.7 | 100.0 | 57.59 |
| PdI: | 0.203 | Peak 2: | 0.000 | 0.0 | 0.000 |
| Intercept: | 0.945 | Peak 3: | 0.000 | 0.0 | 0.000 |
| Result quality : | Good | | | | |

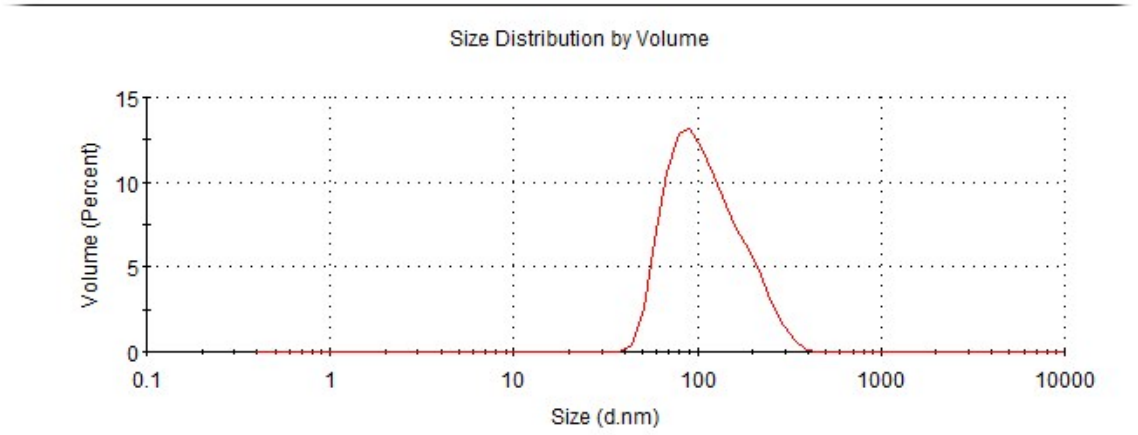


Fig. S3. DLS data for $C_{16}$-Gly-L-Lys measured at 1 mg/mL.

**$C_{16}$-Gly-D-Lys**

| | | | Size (d.nm): | % Volume: | St Dev (d.nm): |
|---|---|---|---|---|---|
| Z-Average (d.nm): | 89.39 | Peak 1: | 82.46 | 98.6 | 50.06 |
| PdI: | 0.303 | Peak 2: | 5000 | 1.4 | 879.4 |
| Intercept: | 0.888 | Peak 3: | 0.000 | 0.0 | 0.000 |
| Result quality : | Refer to quality report | | | | |

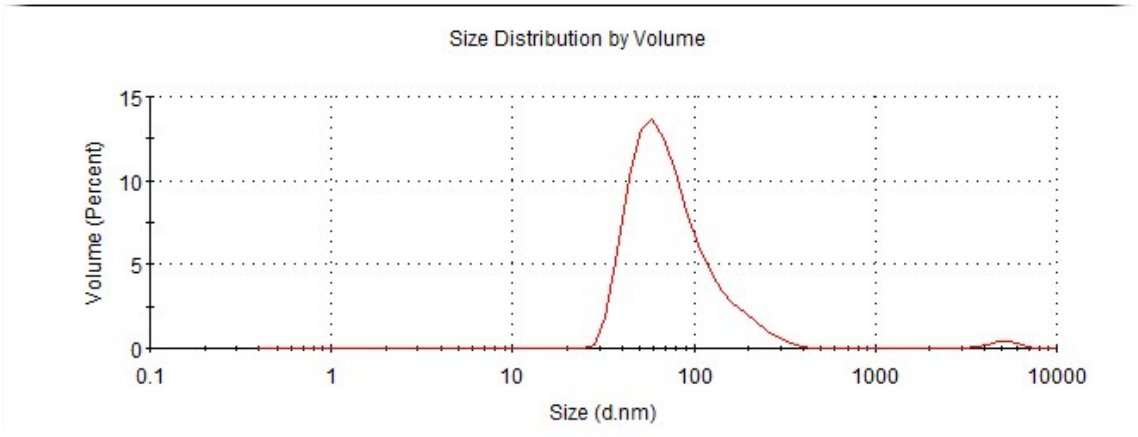


Fig. S4. DLS data for $C_{16}$-Gly-D-Lys measured at 1 mg/mL.

**Effect of Salt on DLS Data**

Larger, less-defined aggregates are observed in the absence of salt.

**$C_{16}$-Gly-L-Lys (no salt)**

| | | Size (d.nm): | % Volume: | St Dev (d.nm): |
|---|---|---|---|---|
| Z-Average (d.nm): 150.1 | Peak 1: | 179.0 | 100.0 | 82.44 |
| PdI: 0.236 | Peak 2: | 0.000 | 0.0 | 0.000 |
| Intercept: 0.963 | Peak 3: | 0.000 | 0.0 | 0.000 |
| Result quality : Good | | | | |

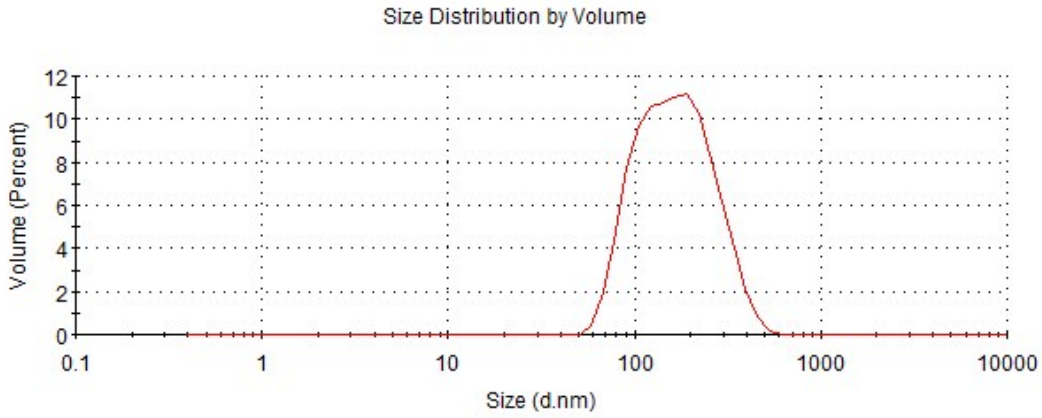


Fig. S5. DLS data for $C_{16}$-Gly-L-Lys (no salt) measured at 1 mg/mL.

**$C_{16}$-Gly-D-Lys (no salt)**

| | | Size (d.nm): | % Volume: | St Dev (d.nm): |
|---|---|---|---|---|
| Z-Average (d.nm): 134.7 | Peak 1: | 148.8 | 100.0 | 73.97 |
| PdI: 0.220 | Peak 2: | 0.000 | 0.0 | 0.000 |
| Intercept: 0.961 | Peak 3: | 0.000 | 0.0 | 0.000 |
| Result quality : Good | | | | |

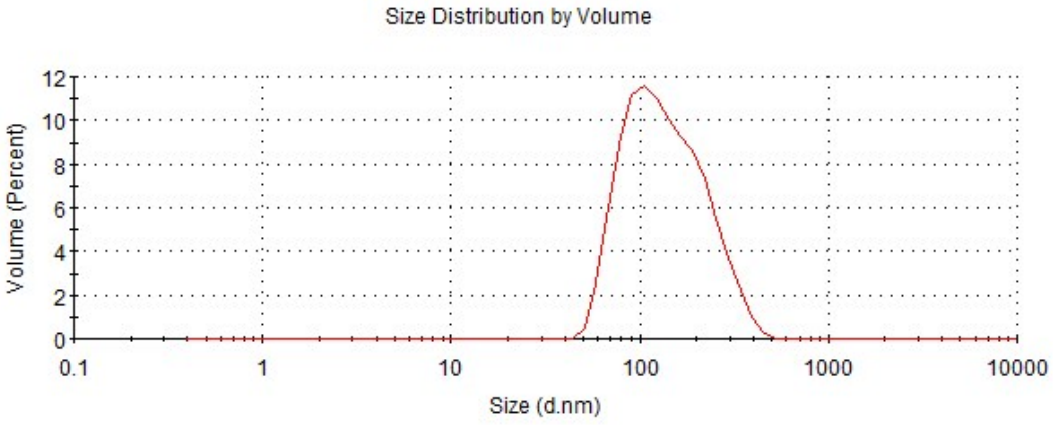


Fig. S6. DLS data for $C_{16}$-Gly-D-Lys (no salt) measured at 1 mg/mL.

**Effect of Concentration on DLS Data**

**C16-Gly-L-Lys (0.5 mg/mL) – Typical Data**

| | | | Size (d.nm): | % Volume: | St Dev (d.nm): |
|---|---|---|---|---|---|
| Z-Average (d.nm): | 106.7 | Peak 1: | 93.05 | 100.0 | 75.23 |
| PdI: | 0.251 | Peak 2: | 0.000 | 0.0 | 0.000 |
| Intercept: | 0.955 | Peak 3: | 0.000 | 0.0 | 0.000 |
| Result quality : | Good | | | | |

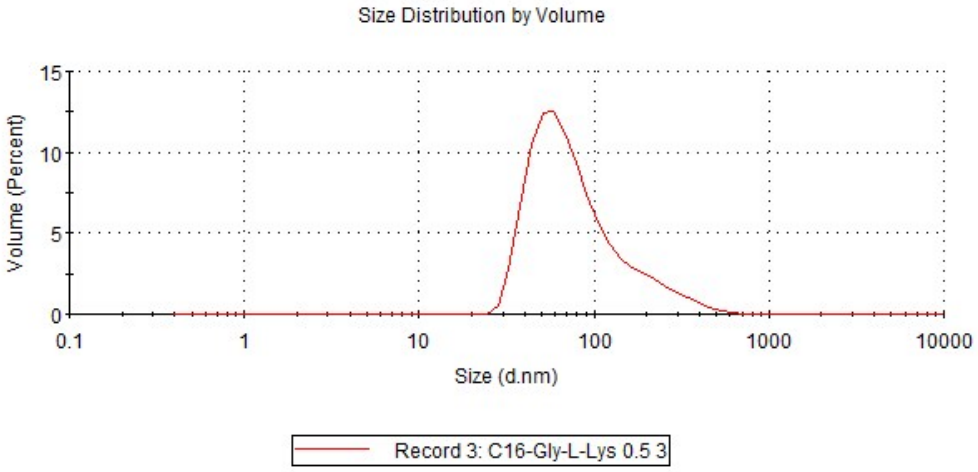


Fig. S7. DLS data for $C_{16}$-Gly-L-Lys measured at 0.5 mg/mL.

**$C_{16}$-Gly-L-Lys (0.25 mg/mL) – Typical Data**

| | | | Size (d.nm): | % Volume: | St Dev (d.nm): |
|---|---|---|---|---|---|
| Z-Average (d.nm): | 129.7 | Peak 1: | 140.1 | 100.0 | 107.4 |
| PdI: | 0.274 | Peak 2: | 0.000 | 0.0 | 0.000 |
| Intercept: | 0.961 | Peak 3: | 0.000 | 0.0 | 0.000 |
| Result quality : | Good | | | | |

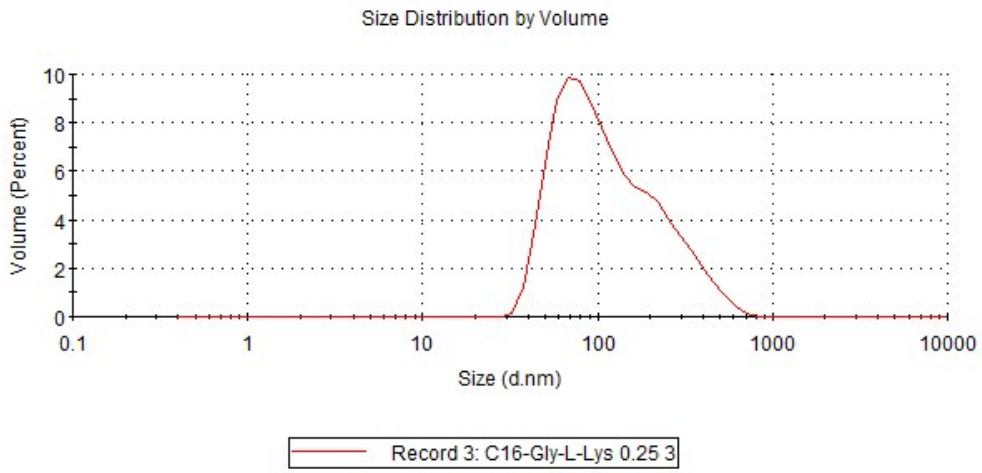


Fig. S8. DLS data for $C_{16}$-Gly-L-Lys measured at 0.5 mg/mL.

**$C_{16}$-Gly-L-Lys (0.125 mg/mL) – Typical Data**

| | | Size (d.nm): | % Volume: | St Dev (d.nm): |
|---|---|---|---|---|
| Z-Average (d.nm): 196.1 | Peak 1: | 272.5 | 20.2 | 139.4 |
| PdI: 0.431 | Peak 2: | 27.89 | 76.7 | 7.871 |
| Intercept: 0.941 | Peak 3: | 5211 | 3.1 | 761.1 |

Result quality : Refer to quality report

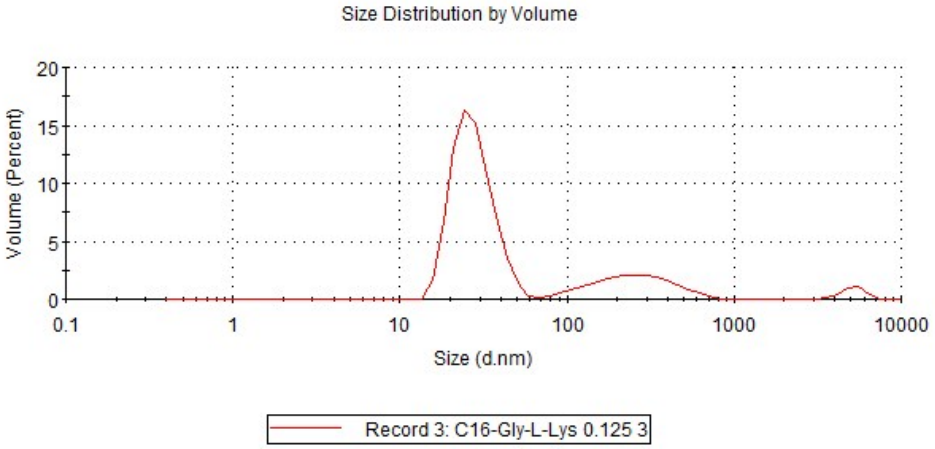


Fig. S9. DLS data for $C_{16}$-Gly-L-Lys measured at 0.125 mg/mL.

**$C_{16}$-Gly-L-Lys (0.05 mg/mL)**

All three plots are shown as there is significant variation at this low concentration

| | | Size (d.nm): | % Volume: | St Dev (d.nm): |
|---|---|---|---|---|
| Z-Average (d.nm): 122.7 | Peak 1: | 147.8 | 5.2 | 53.67 |
| PdI: 0.305 | Peak 2: | 15.78 | 94.8 | 3.370 |
| Intercept: 0.877 | Peak 3: | 0.000 | 0.0 | 0.000 |

Result quality : Refer to quality report

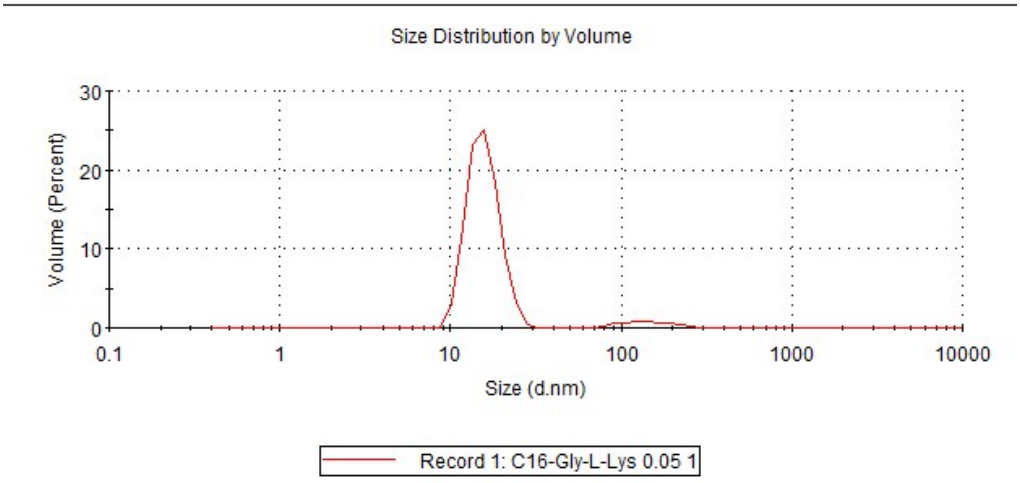


Fig. S10. DLS data for $C_{16}$-Gly-L-Lys measured at 0.05 mg/mL (run 1).

| | | Size (d.nm): | % Volume: | St Dev (d.nm): |
|---|---|---|---|---|
| Z-Average (d.nm): 117.1 | Peak 1: | 9.858 | 85.7 | 2.281 |
| PdI: 0.424 | Peak 2: | 43.84 | 12.6 | 31.47 |
| Intercept: 0.876 | Peak 3: | 299.1 | 1.7 | 128.8 |

Result quality : Good

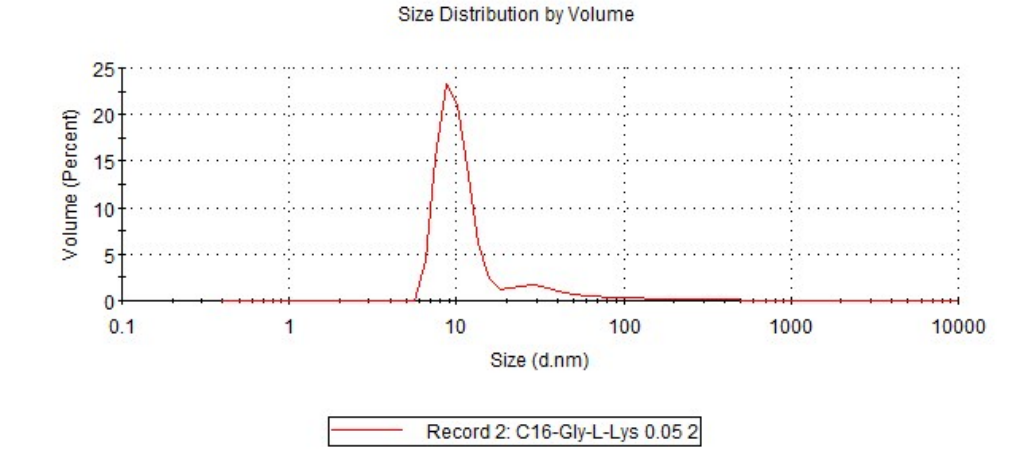


Fig. S11. DLS data for $C_{16}$-Gly-L-Lys measured at 0.05 mg/mL (run 2).

| | | Size (d.nm): | % Volume: | St Dev (d.nm): |
|---|---|---|---|---|
| Z-Average (d.nm): 105.6 | Peak 1: | 47.96 | 100.0 | 75.49 |
| PdI: 0.458 | Peak 2: | 0.000 | 0.0 | 0.000 |
| Intercept: 0.879 | Peak 3: | 0.000 | 0.0 | 0.000 |
| Result quality : Good | | | | |

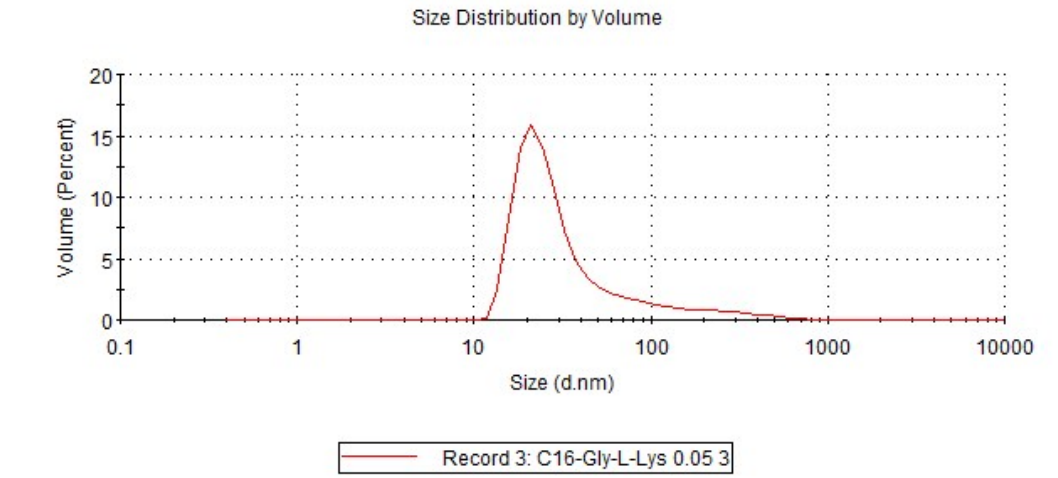


Fig. S12. DLS data for $C_{16}$-Gly-L-Lys measured at 0.05 mg/mL (run 3).

**$C_{16}$-Gly-D-Lys (0.5 mg/mL) – Typical Data**

| | | Size (d.nm): | % Volume: | St Dev (d.nm): |
|---|---|---|---|---|
| Z-Average (d.nm): 140.1 | Peak 1: | 141.4 | 91.5 | 94.84 |
| PdI: 0.362 | Peak 2: | 4878 | 8.5 | 955.5 |
| Intercept: 0.956 | Peak 3: | 0.000 | 0.0 | 0.000 |
| Result quality : Good | | | | |

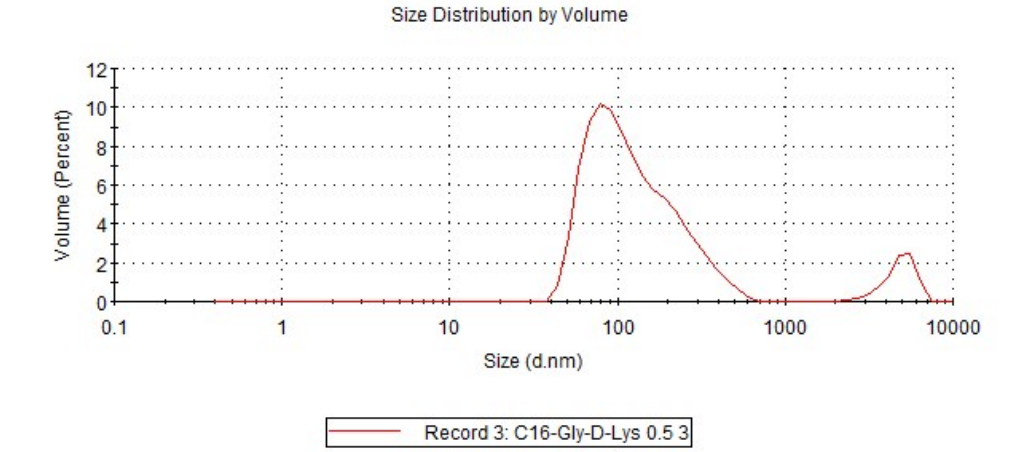


Fig. S13. DLS data for $C_{16}$-Gly-D-Lys measured at 0.5 mg/mL.

**$C_{16}$-Gly-D-Lys (0.25 mg/mL) – Typical Data**

| | | Size (d.nm): | % Volume: | St Dev (d.nm): |
|---|---|---|---|---|
| Z-Average (d.nm): 112.8 | Peak 1: | 52.35 | 88.0 | 30.91 |
| PdI: 0.399 | Peak 2: | 275.4 | 12.0 | 105.3 |
| Intercept: 0.960 | Peak 3: | 0.000 | 0.0 | 0.000 |
| Result quality : Good | | | | |

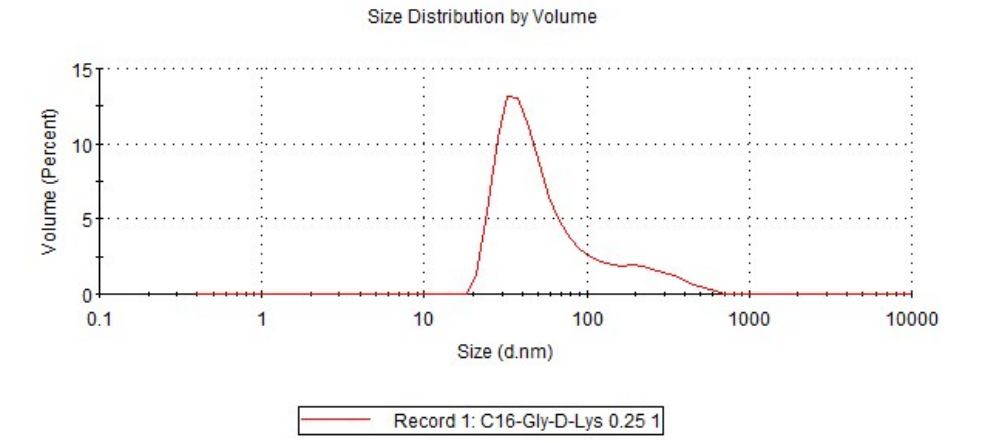


Fig. S14. DLS data for $C_{16}$-Gly-D-Lys measured at 0.25 mg/mL.

**$C_{16}$-Gly-D-Lys (0.125 mg/mL)**

All three plots are shown as there is significant variation

| | | Size (d.nm): | % Volume: | St Dev (d.nm): |
|---|---|---|---|---|
| Z-Average (d.nm): 116.4 | Peak 1: | 53.60 | 10.9 | 68.51 |
| PdI: 0.438 | Peak 2: | 8.338 | 89.0 | 1.934 |
| Intercept: 0.942 | Peak 3: | 5194 | 0.1 | 768.3 |
| Result quality : Good | | | | |

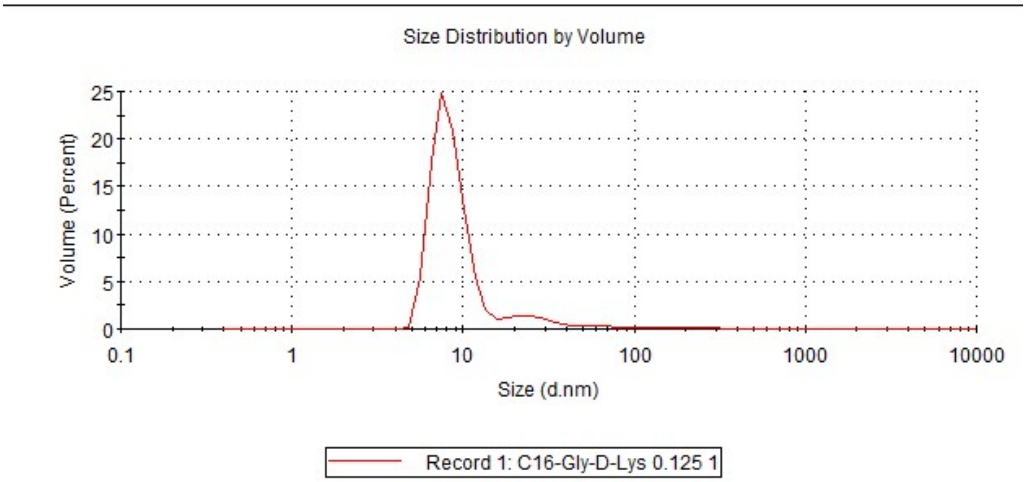


Fig. S15. DLS data for $C_{16}$-Gly-D-Lys measured at 0.125 mg/mL (run 1).

| | | Size (d.nm): | % Volume: | St Dev (d.nm): |
|---|---|---|---|---|
| Z-Average (d.nm): 114.2 | Peak 1: | 124.6 | 96.5 | 121.2 |
| PdI: 0.443 | Peak 2: | 5050 | 3.5 | 851.8 |
| Intercept: 0.938 | Peak 3: | 0.000 | 0.0 | 0.000 |
| Result quality : Good | | | | |

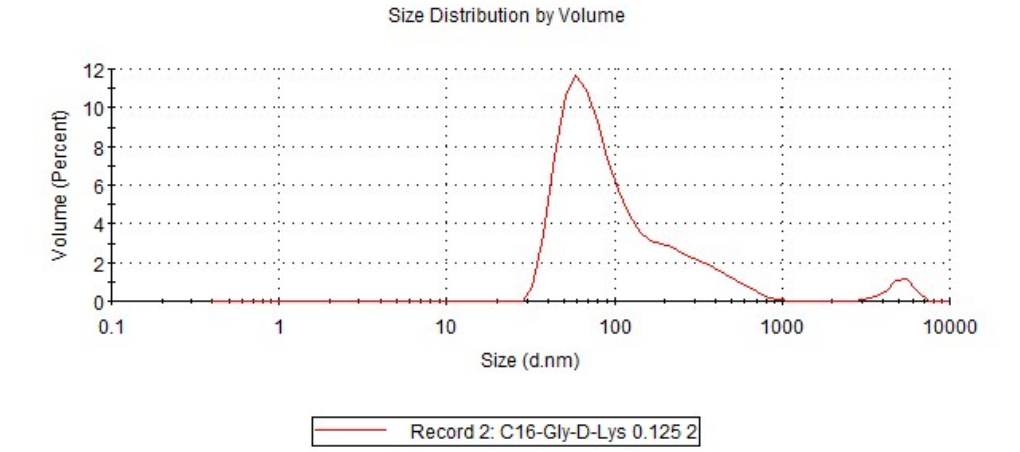


Fig. S16. DLS data for $C_{16}$-Gly-D-Lys measured at 0.125 mg/mL (run 2).

| | | | Size (d.nm): | % Volume: | St Dev (d.nm): |
|---|---|---|---|---|---|
| Z-Average (d.nm): | 113.3 | Peak 1: | 49.22 | 84.5 | 25.54 |
| PdI: | 0.458 | Peak 2: | 274.0 | 14.3 | 122.2 |
| Intercept: | 0.936 | Peak 3: | 5258 | 1.2 | 737.9 |

Result quality : Refer to quality report

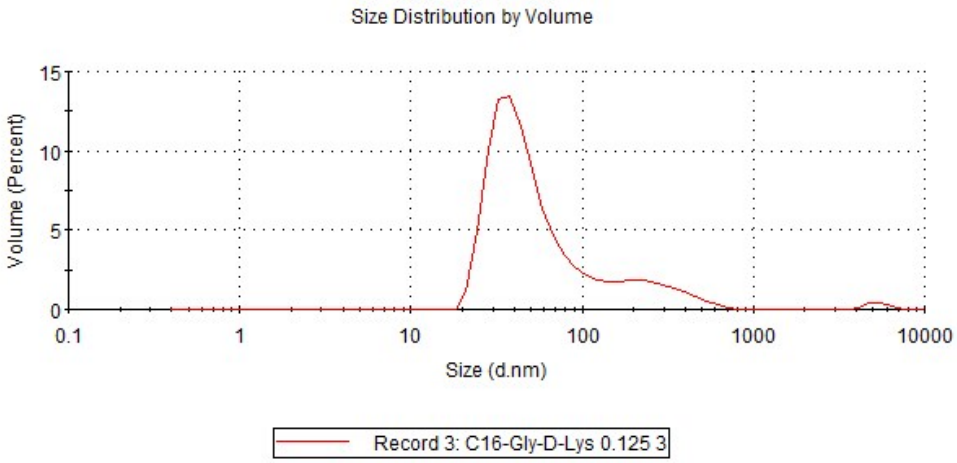


Fig. S17. DLS data for $C_{16}$-Gly-D-Lys measured at 0.125 mg/mL (run 3).

**$C_{16}$-Gly-D-Lys (0.05 mg/mL)**

All three plots are shown as there is significant variation at this low concentration

| | | Size (d.nm): | % Volume: | St Dev (d.nm): |
|---|---|---|---|---|
| Z-Average (d.nm): 76.93 | Peak 1: | 72.74 | 6.6 | 33.03 |
| PdI: 0.254 | Peak 2: | 15.88 | 93.4 | 4.880 |
| Intercept: 0.772 | Peak 3: | 0.000 | 0.0 | 0.000 |

Result quality : Refer to quality report

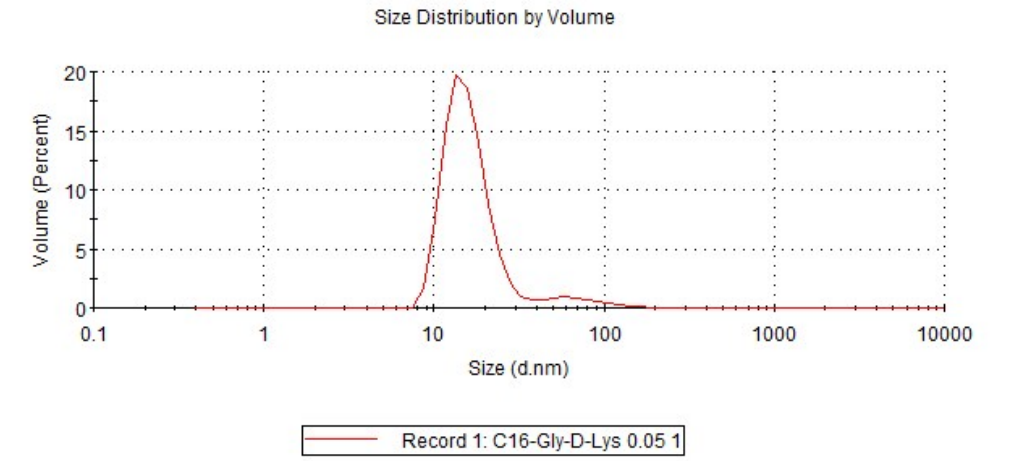


Fig. S18. DLS data for $C_{16}$-Gly-D-Lys measured at 0.05 mg/mL (run 1).

| | | Size (d.nm): | % Volume: | St Dev (d.nm): |
|---|---|---|---|---|
| Z-Average (d.nm): 55.97 | Peak 1: | 14.81 | 99.9 | 13.64 |
| PdI: 0.460 | Peak 2: | 5300 | 0.1 | 714.0 |
| Intercept: 0.733 | Peak 3: | 0.000 | 0.0 | 0.000 |

Result quality : Good

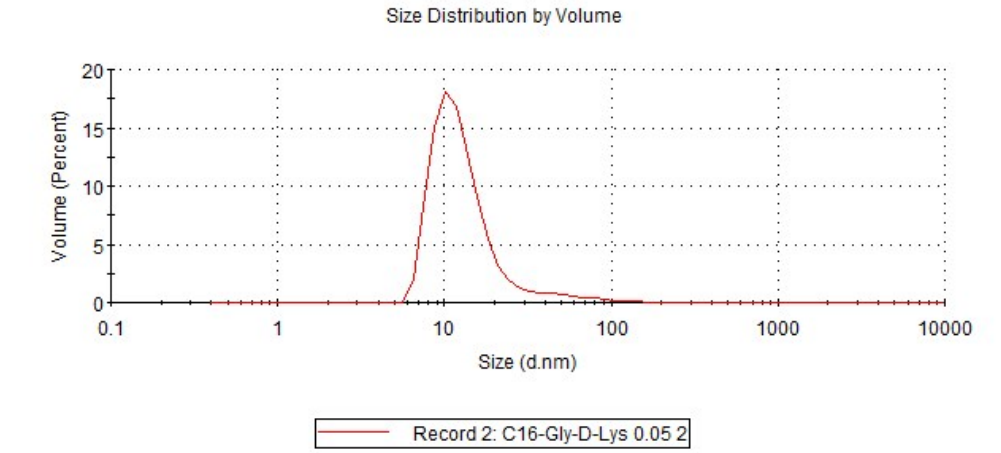


Fig. S19. DLS data for $C_{16}$-Gly-D-Lys measured at 0.05 mg/mL (run 2).

| | | Size (d.nm): | % Volume: | St Dev (d.nm): |
|---|---|---|---|---|
| Z-Average (d.nm): 56.48 | Peak 1: | 9.643 | 100.0 | 10.59 |
| PdI: 0.474 | Peak 2: | 5272 | 0.0 | 730.6 |
| Intercept: 0.726 | Peak 3: | 0.000 | 0.0 | 0.000 |

Result quality : Good

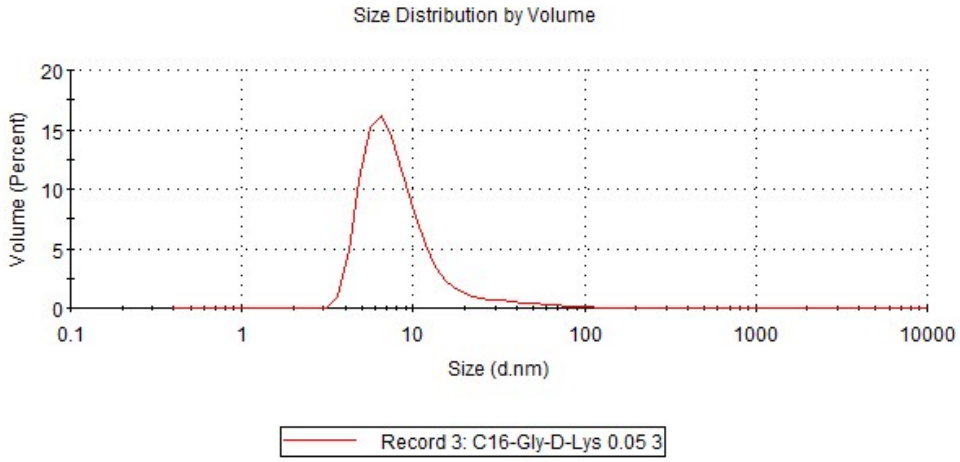


Fig. S20. DLS data for $C_{16}$-Gly-D-Lys measured at 0.05 mg/mL (run 3).

## 4. Circular Dichroism Data

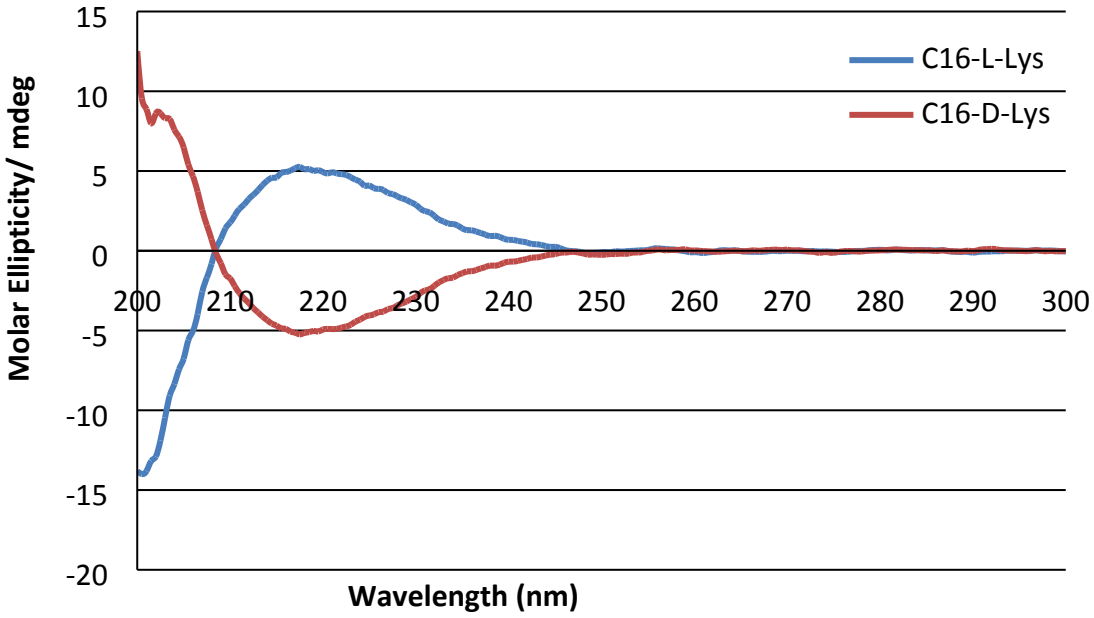


Fig. S21. CD spectra of $C_{16}$-L-Lys and $C_{16}$-D-Lys (1 mg/mL in 10 mM HEPES buffer)

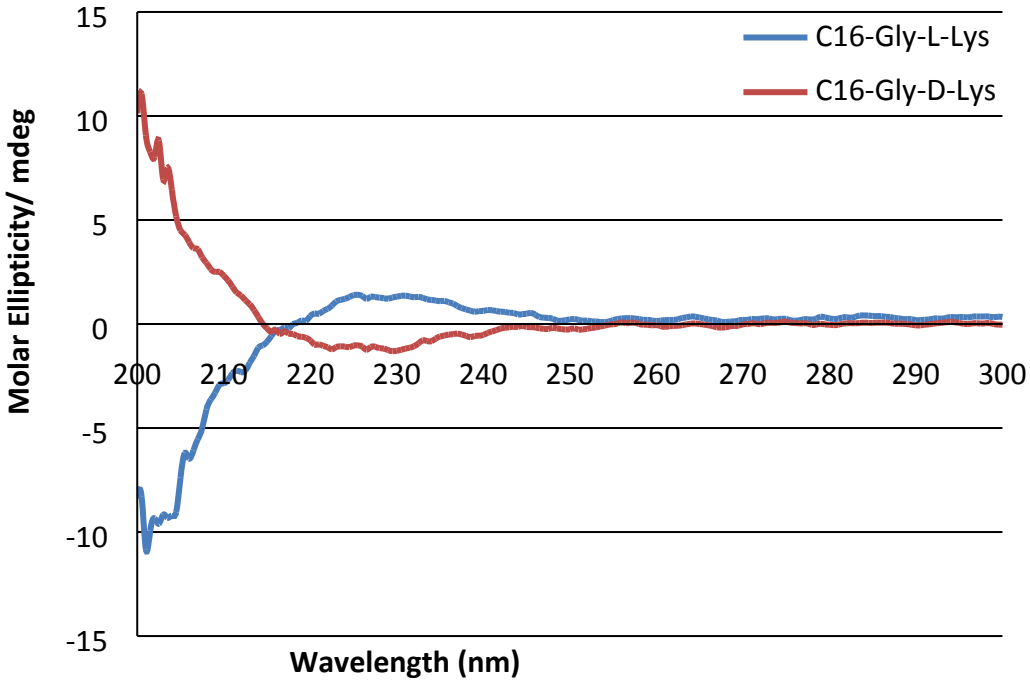


Fig. S22. CD spectra of $C_{16}$-Gly-L-Lys and $C_{16}$-Gly-D-Lys (1 mg/mL in 10 mM HEPES buffer)

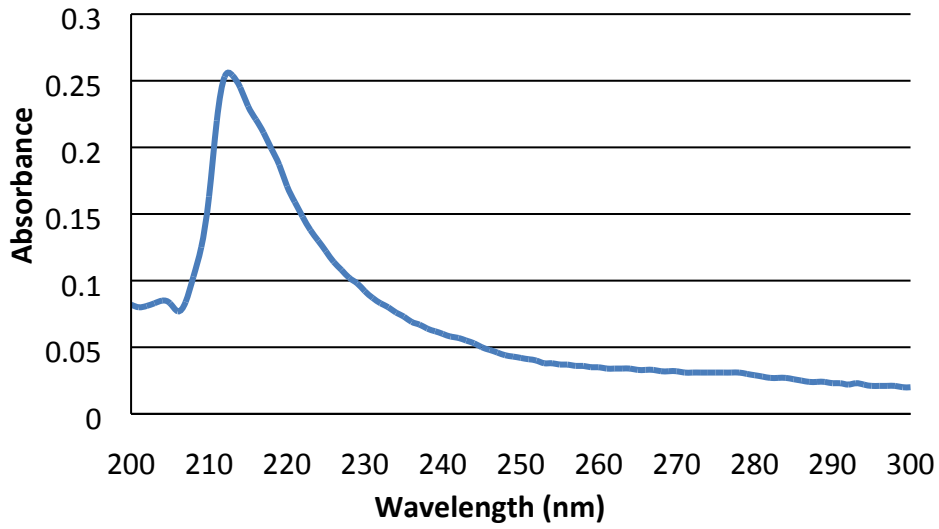


Fig. S23. UV-Vis Absorption spectra of $C_{16}$-L-Lys (1 mg/mL in 10mM HEPES buffer)

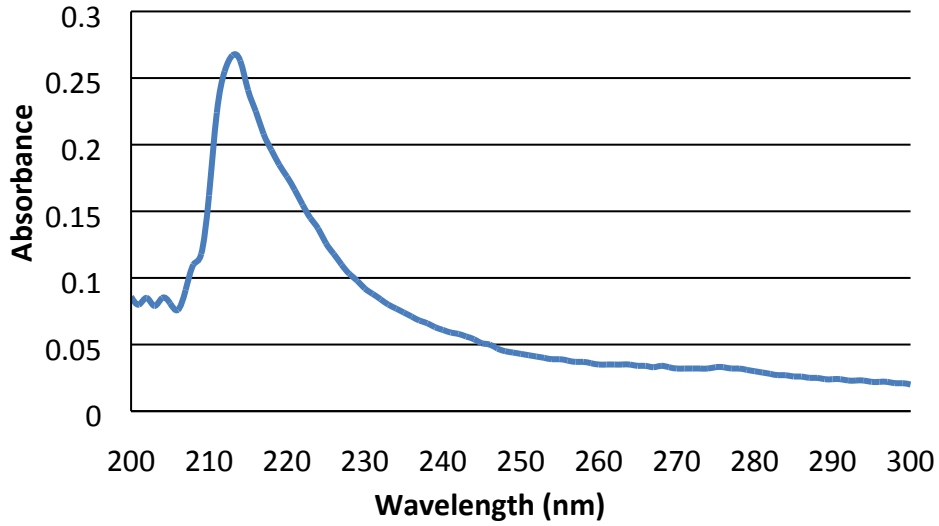


Fig. S24. UV-Vis Absorption spectra of $C_{16}$-Gly-L-Lys (1 mg/mL in 10mM HEPES buffer)

## 5. Critical Aggregation Concentrations (CACs) Determined by Nile Red Assay

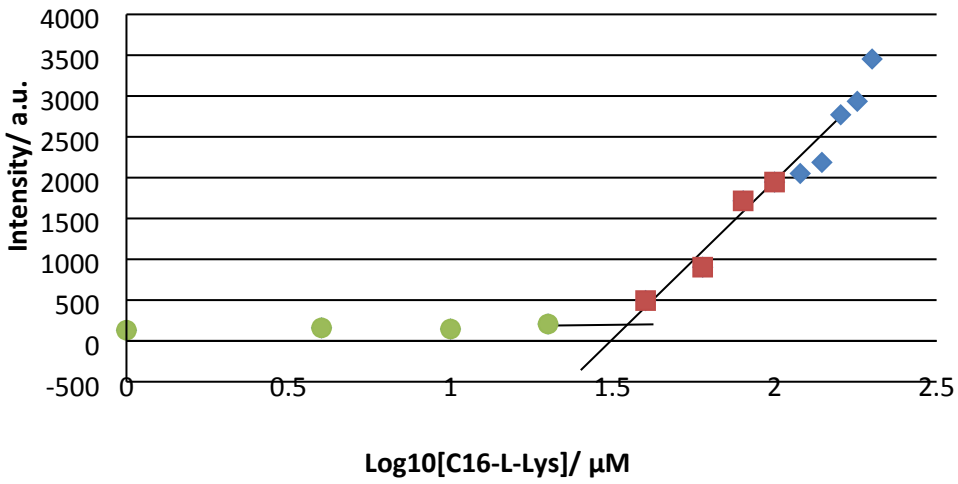


Fig. S25. Fluorescence intensity of Nile Red in the presence of increasing amounts of $C_{16}$-L-Lys

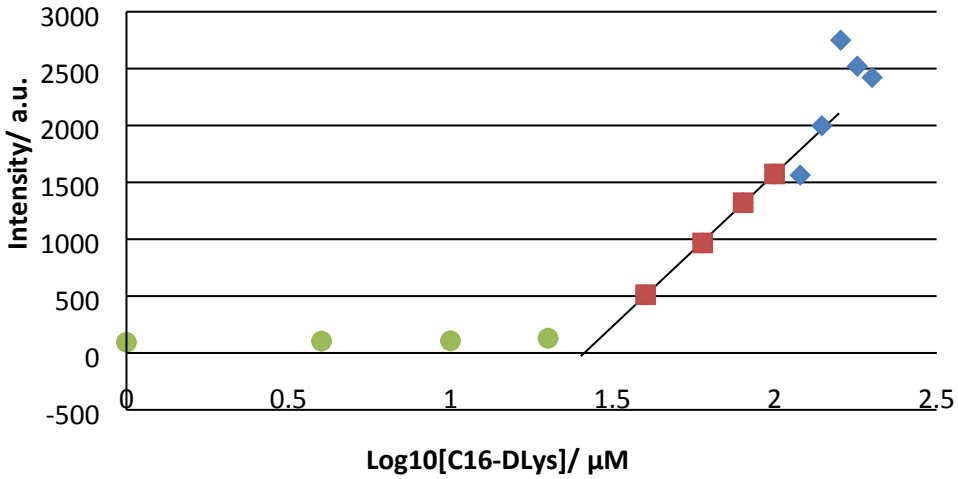


Fig. S26. Fluorescence intensity of Nile Red in the presence of increasing amounts of $C_{16}$-D-Lys

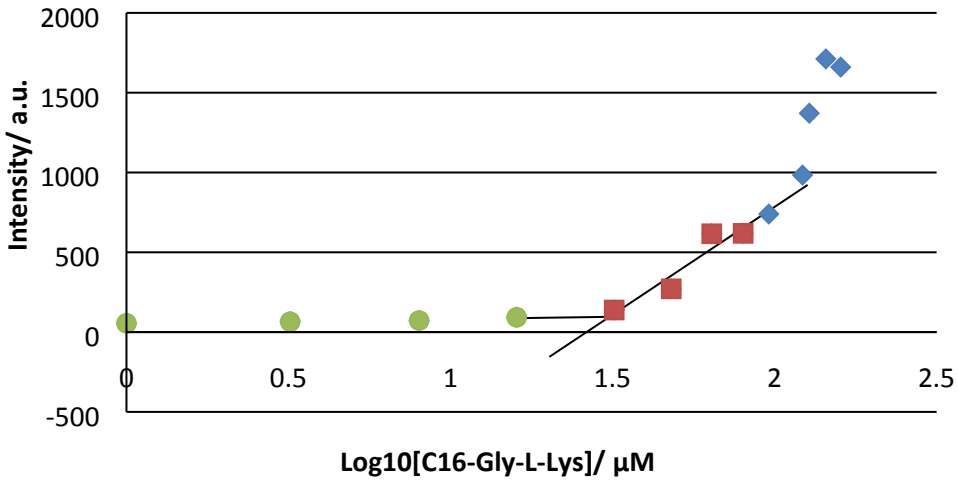


Fig. S27. Fluorescence intensity of Nile Red in the presence of increasing amounts of $C_{16}$-Gly-L-Lys

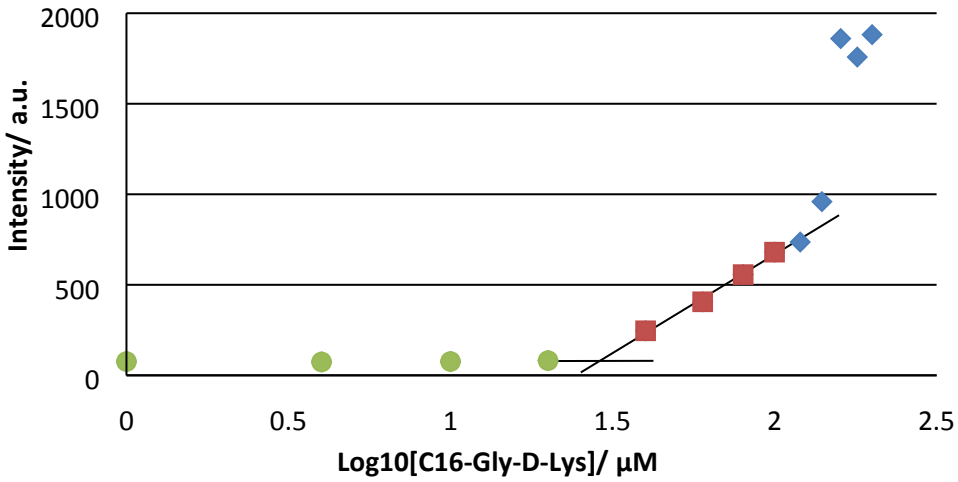


Fig. S28. Fluorescence intensity of Nile Red in the presence of increasing amounts of $C_{16}$-Gly-L-Lys

## 6 Transmission Electron Microscopy Images

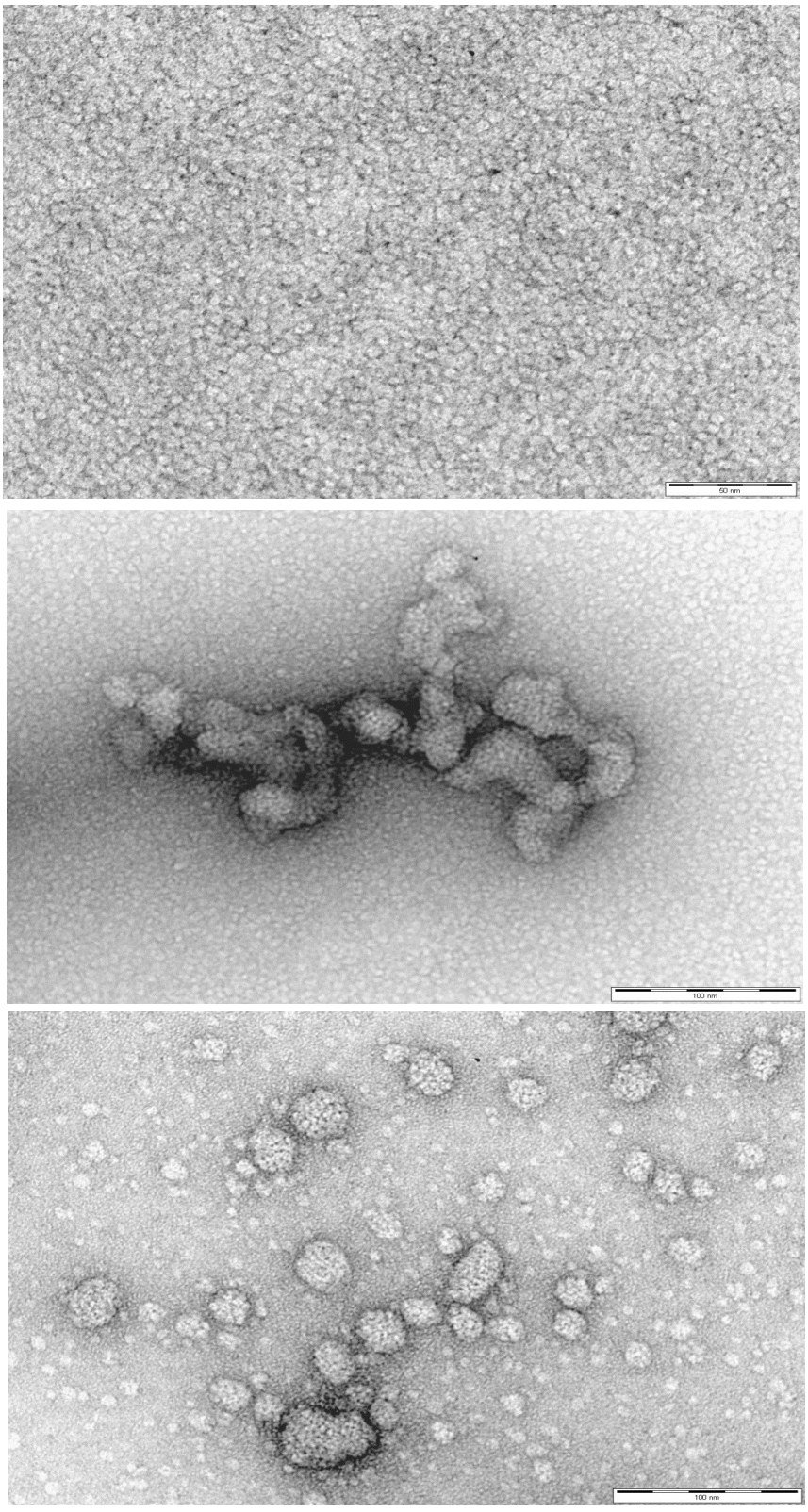


Fig. S29. TEM images of $C_{16}$-D-Lys in the absence (top) and presence of heparin (middle) and DNA (bottom).

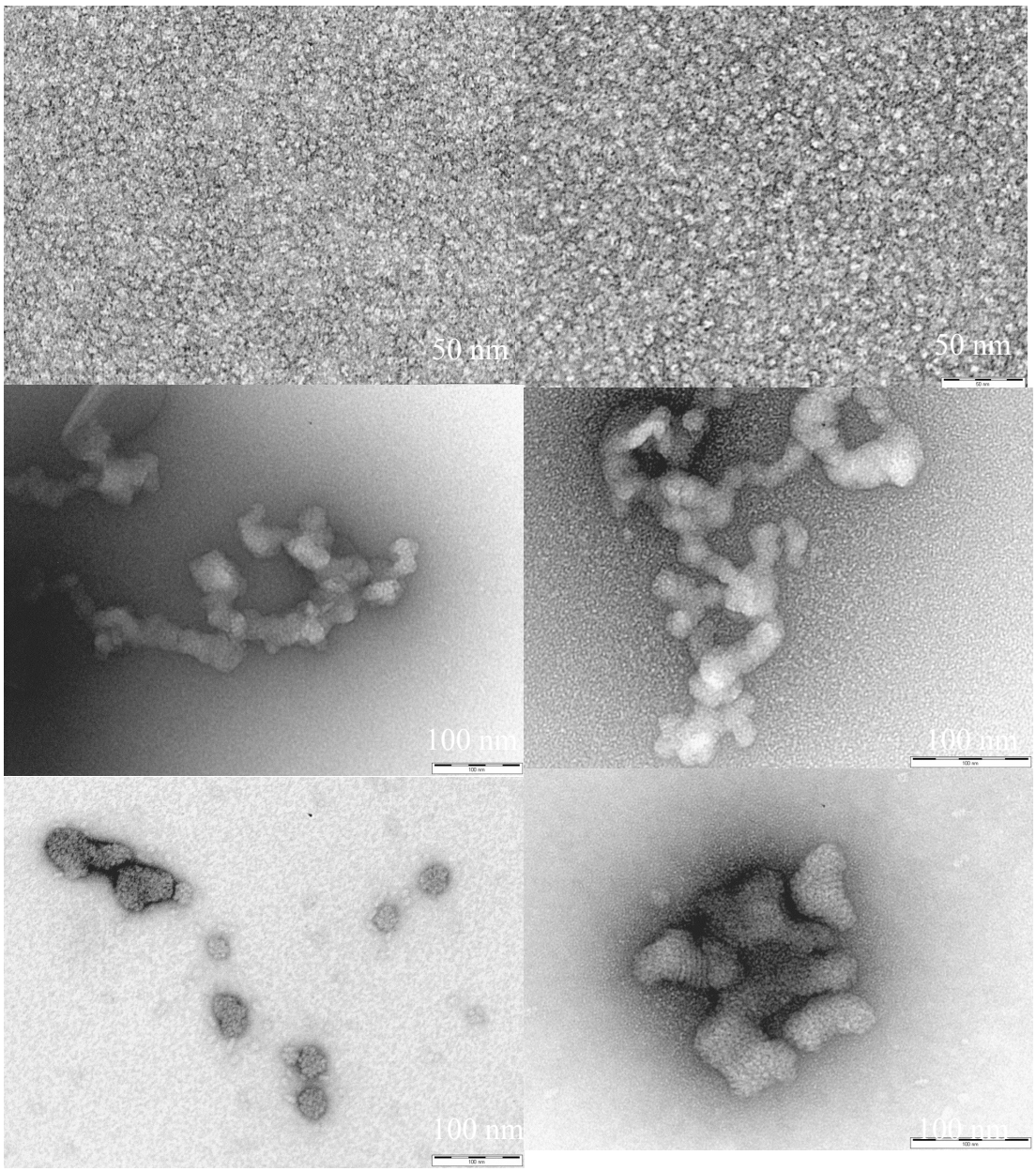


Fig. S30. TEM images of $C_{16}$-Gly-L-Lys (left) and $C_{16}$-Gly-D-Lys (right) in the absence (top) and presence of heparin (middle) and DNA (bottom).

## 7. NMR Spectra of Target Compounds

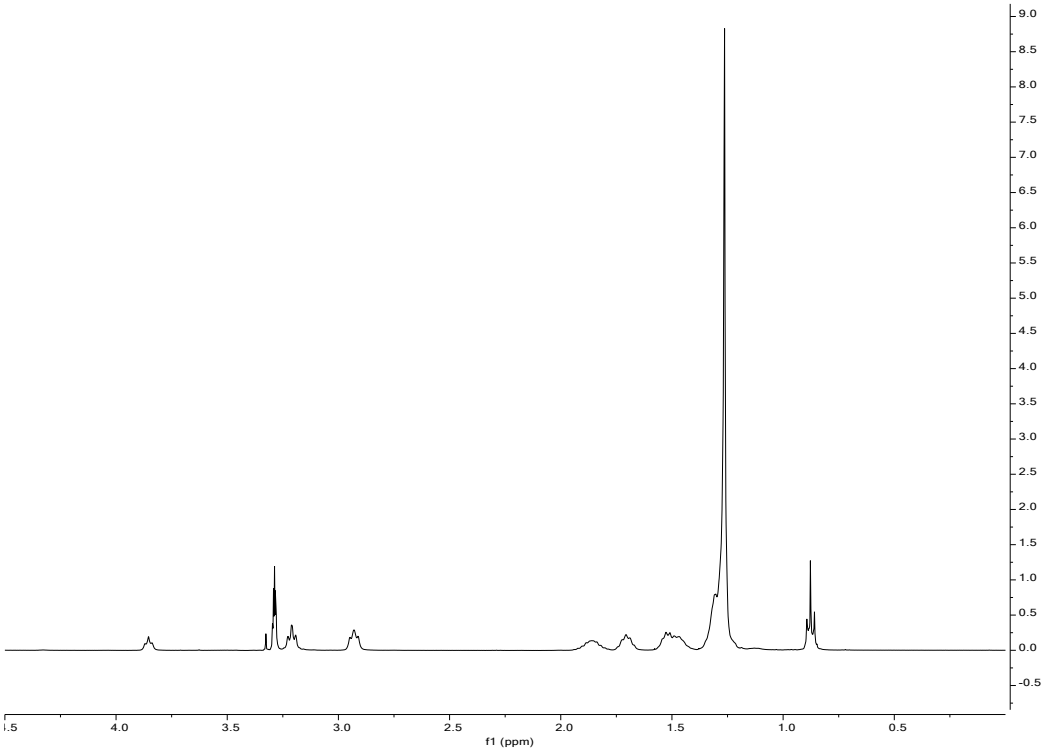


Fig. S31. $^{1}H$ NMR spectrum of $C_{16}$-L-Lys measured in $CD_3OD$.

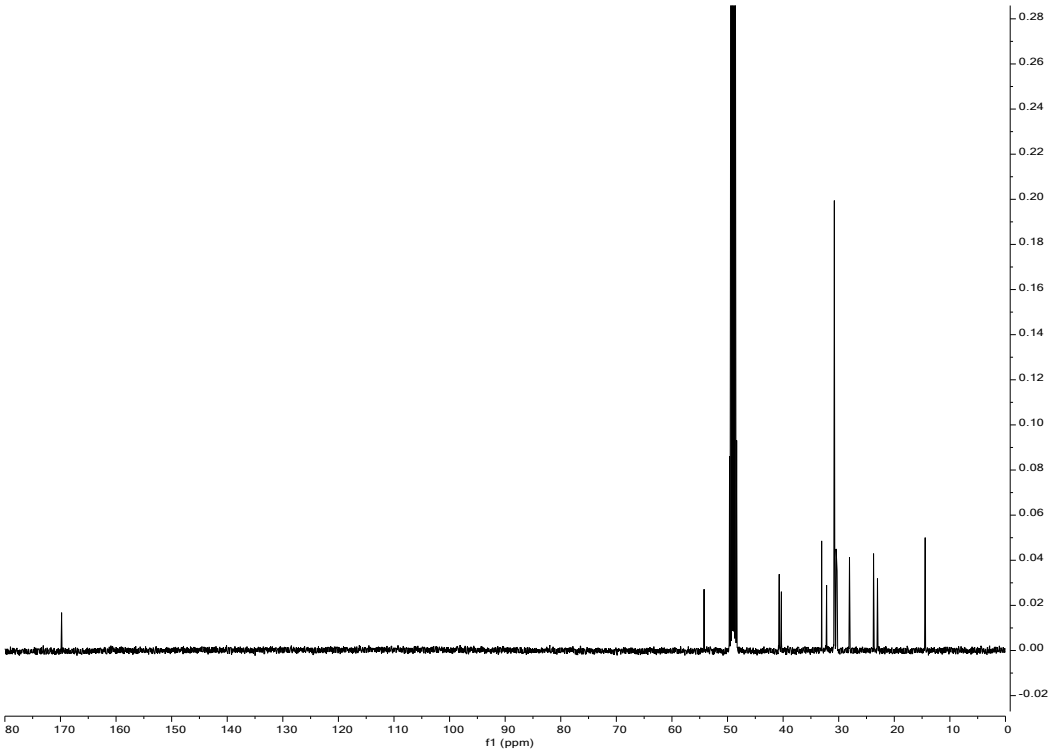


Fig. S32. $^{13}C$ NMR spectrum of $C_{16}$-L-Lys measured in $CD_3OD$.

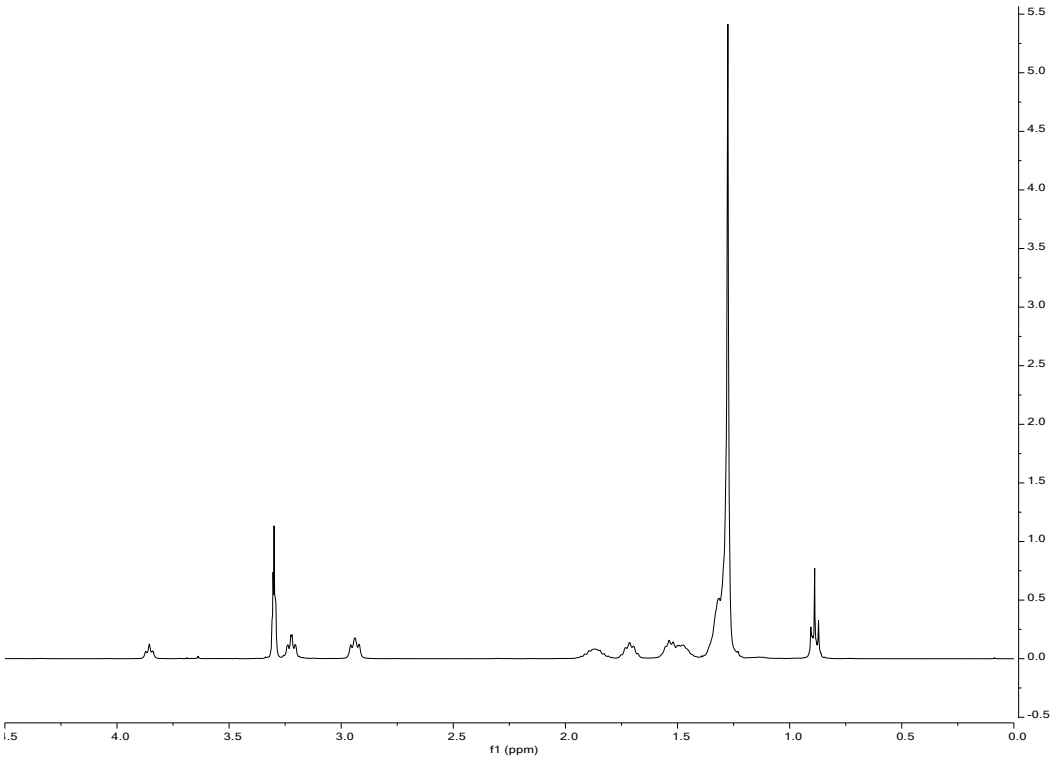


Fig. S33. $^{1}H$ NMR spectrum of $C_{16}$-D-Lys measured in $CD_3OD$.

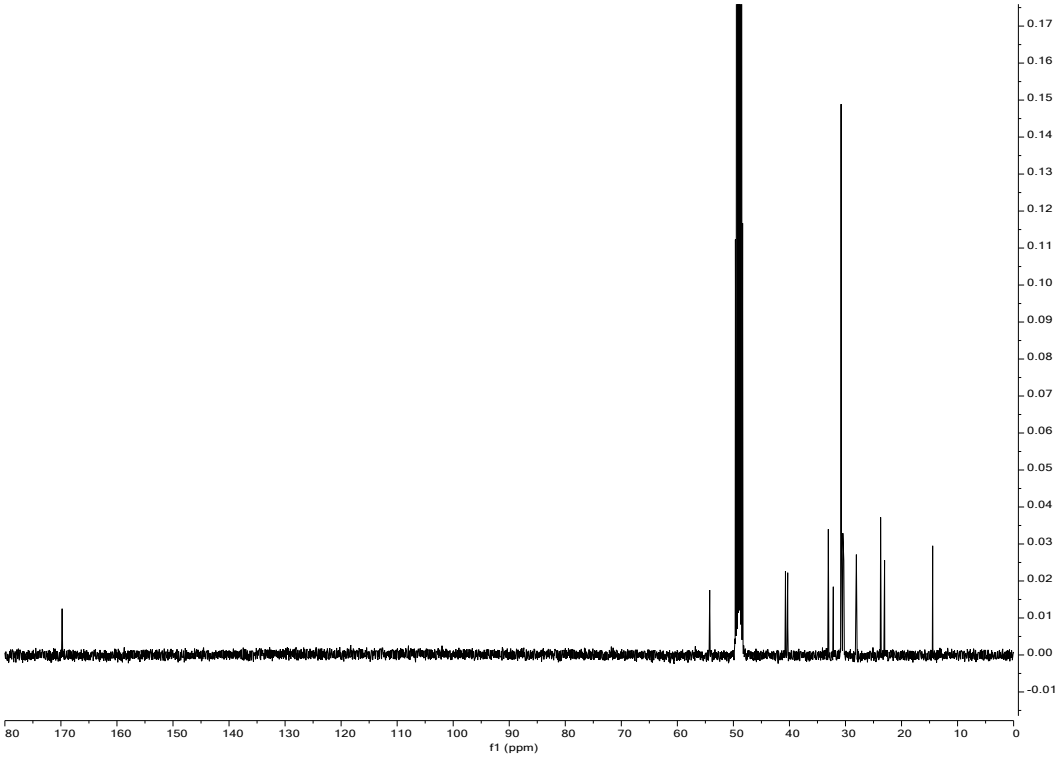


Fig. S34. $^{13}C$ NMR spectrum of $C_{16}$-L-Lys measured in $CD_3OD$.

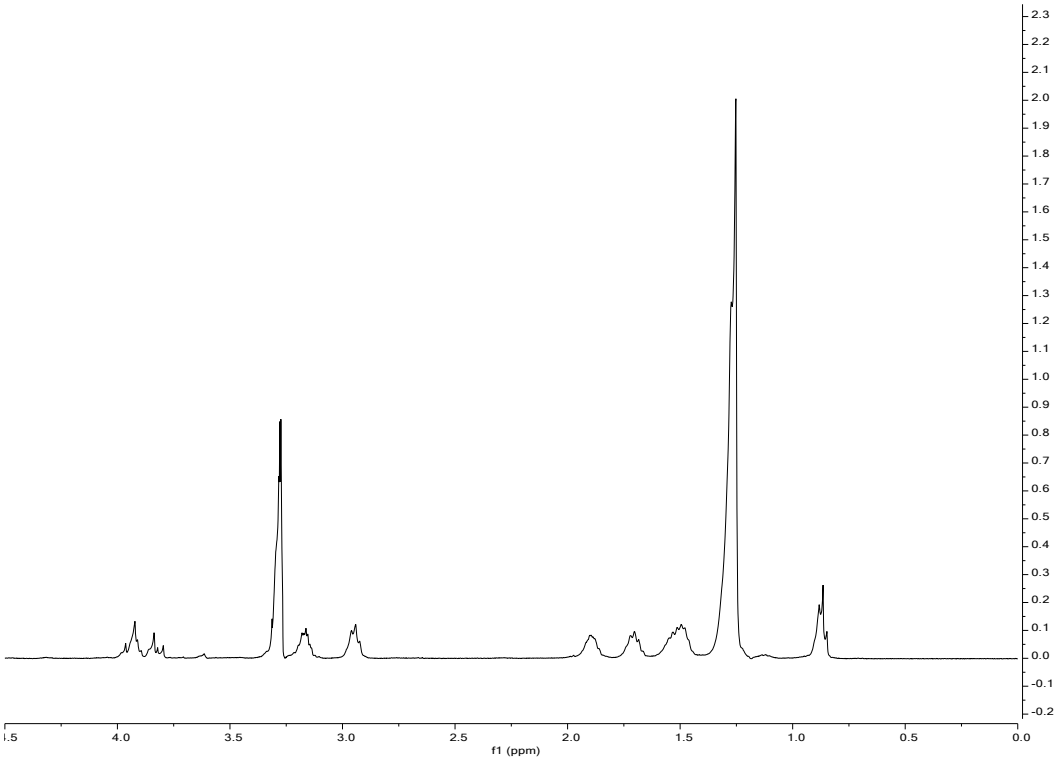


Fig. S35. $^{1}H$ NMR spectrum of $C_{16}$-Gly-L-Lys measured in $CD_3OD$.

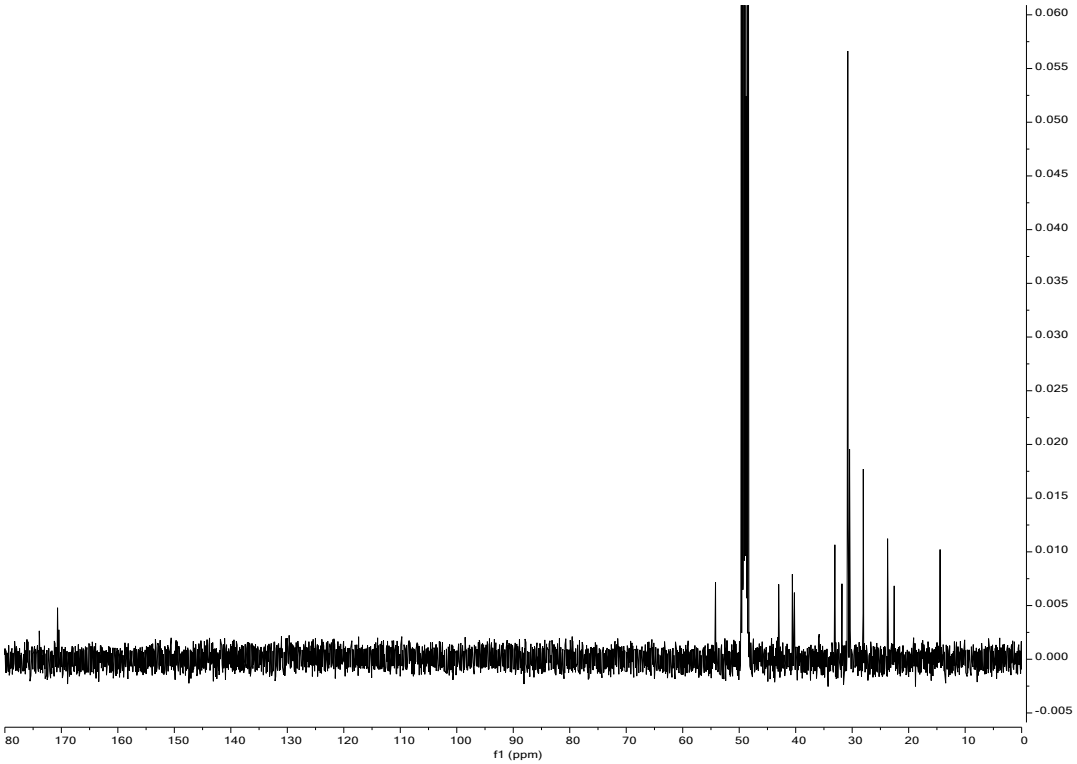


Fig. S36. $^{13}C$ NMR spectrum of $C_{16}$-Gly-L-Lys measured in $CD_3OD$.

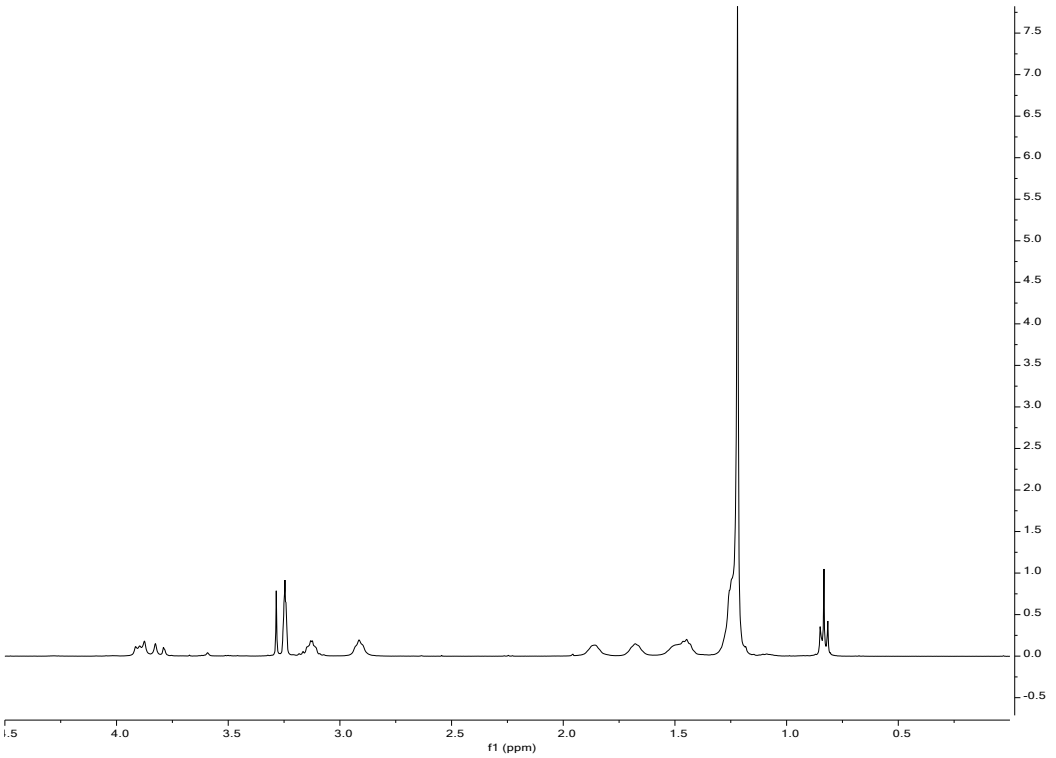


Fig. S37. $^{1}H$ NMR spectrum of $C_{16}$-Gly-D-Lys measured in $CD_3OD$.

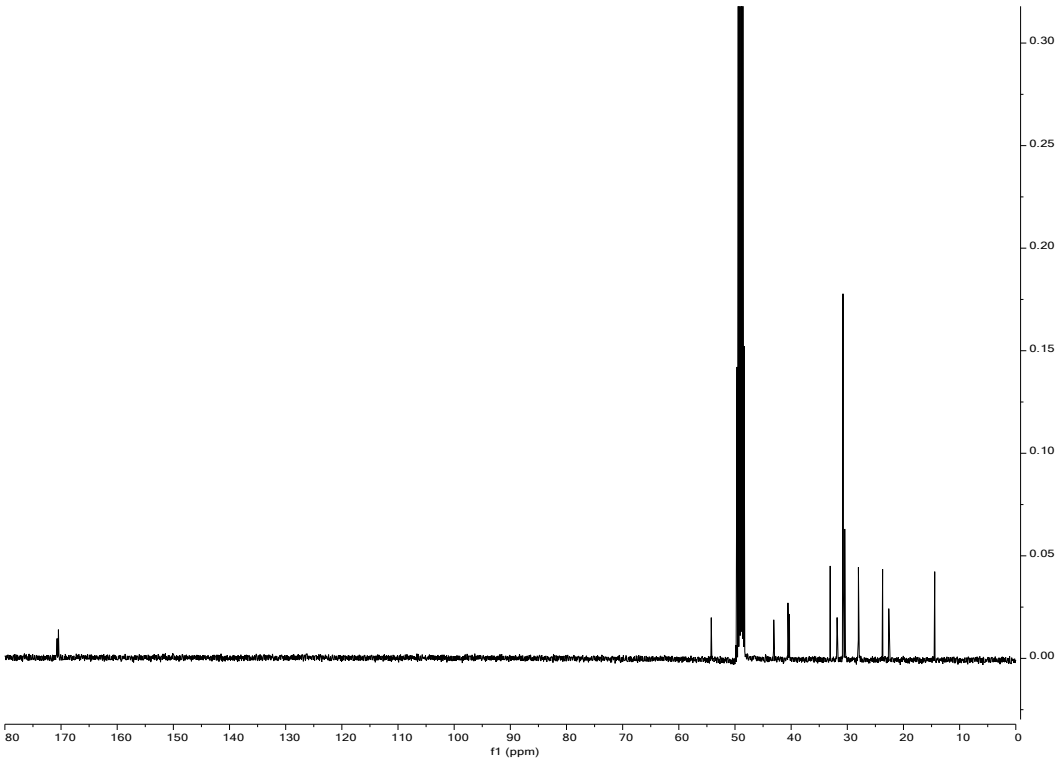


Fig. S38. $^{13}C$ NMR spectrum of $C_{16}$-Gly-D-Lys measured in $CD_3OD$.

## 8. Competition Assay Methods

### 8.1 Nile Red Encapsulation[1]

A 2.5 mM Nile Red stock solution was made in EtOH. A dendron stock solution was made up in PBS/SHE buffer at various concentrations. Aliquots of the stock solution were taken and diluted with PBS/SHE to the desired concentration in a 1 ml assay volume in cuvette. Nile red (1 µl) was added and the cuvettes were placed in 45 $^{o}$C water bath at least 10 minutes before the measurement. The fluorescence emission was measured on a Hitachi F-4500 spectrofluorimeter using an excitation wavelength of 363 nm. The fluorescence intensity of the excimer band was recorded at 495 nm. The discontinuity in excimer intensity with concentration was considered to represent the critical aggregation concentration. Experiments were performed in triplicate.

### 8.2 Ethidium Bromide Displacement[2, 3]

A solution of Calf Thymus DNA (8.0 µM) was prepared in SHE Buffer (2 mM HEPES, 0.05 mM EDTA, 150mM NaCl) at pH 7.5. Ethidium bromide was diluted with SHE Buffer to give a final concentration of 10.14 µM. Background ethidium bromide fluorescence was measured at 5.07 µM. The dendron stock solution, at varying concentration depending on the charge of the dendron, was prepared in a 50:50 solution of the ethidium bromide and DNA solutions to give a final EthBr concentration of 5.07 µM and DNA at 4.0 µM with respect to one DNA base (*Mr* 330 gmol$^{-1}$). Appropriate amounts of the dendron solution were added to 2 ml of a stock containing EthBr (5.07 µM) and DNA (4.0 µM) to achieve the desired N:P ratio. The fluorescence was measured on a Hitachi F-4500 spectrofluorimeter using an excitation wavelength of 540 nm. Fluorescence intensity was recorded at 595 nm. The fluorescence values were normalised to a solution containing only DNA (4.0 µM) and EthBr (5.07 µM). Experiments were performed in triplicate.

### 8.3 Heparin Displacement Assay using Mal-B In Buffer[4]

A cuvette containing 2 mL of MalB (25 µM), heparin (27 µM) and NaCl (150 mM) in Tris

HCl (10 mM) was titrated with binder stock solution to give the cuvette suitable binder-heparin charge ratios. The binder stock solution was composed of the original MalB/heparin/NaCl/Tris HCl stock solution endowed additionally with a concentration of binder such that, after addition of 10 μL binder stock, the cuvette charge ratio (+ : –) is increased by 0.037. After each addition, the cuvette was inverted to ensure good mixing and the absorbance at 615 nm was recorded against a Tris HCl (10 mM) baseline. Absorbance was normalised between a solution of MalB (25 μM), NaCl (150 mM) in Tris HCl (10 mM) and one containing MalB (25 μM), heparin (27 μM), NaCl (150 mM) in Tris HCl (10 mM).

**9. Isothermal Titration Calorimetry**

Isothermal titration calorimetry (ITC) experiments were performed with a MicroCal PEAQ-ITC calorimeter (Malvern, UK) at 25°C. The cell volume was 280 μL. All experiments were conducted in a forward manner, that is, by step-by-step injections of a constant volume of concentrated SAMul solutions into the calorimetric cell containing buffer (Tris HCl 10 mM/150 mM NaCl), or buffered solutions of heparin or DNA, respectively. Specifically, for CAC determination, a series of SAMul solutions of 1 mM were injected in 77 portions with a 0.5 μL syringe at 150 s intervals. For heparin and DNA binding, a series of SAMul solution of 10 mM were injected in 39 portions with a 1 μL syringe at 150 s intervals, such that the SAMul system was always above the critical aggregation concentration (CAC). The polyanion concentration in the calorimeter cell was 500 μM. All solutions and buffer were degassed for 30 min at room temperature under stirring at 500 rpm prior to each experiment. After careful washing, the cell was pre-rinsed with a portion of the buffer, heparin or DNA solutions. Upon filling cell and syringe, stirring was turned on and the system was allowed to thermally equilibrate for 30 minutes.

During polyanion/SAMul binding experiments, when all binding sites were occupied, only a heat signal resulting from mixing, dilution effects and liquid friction was observed. The values of these non-specific heats were further confirmed by control experiments (data not shown); accordingly, they were subtracted from the relevant data set to yield the corrected integrated data.

For critical micelle concentration (CMC) determination, the demicellization thermograms of all four SAMul molecules titrated into buffer solution were effectively the same. Figure S39 shows the data obtained for $C_{16}$-D-Lys as an example. The injection of each concentrated SAMul solution into the buffer mostly resulted in large, exothermic signals, followed by a series of small, endothermic peaks in the later stages of the experiment (Figure S39, insert). The enthalpy change characterizing the first part of the thermogram, corresponding to the addition of the SAMul stock solution (which, for each systems, was always higher than the corresponding CMC) to the buffer, is due to demicellization, micelle dilution, and dilution of the surfactant monomer. The variation in enthalpy observed toward the end of the titration is mainly associated with micellar dilution, with the SAMul concentration in the cell being well above the corresponding CMC. Subtraction of the micelle dilution heat, normalization per mol of SAMul, and integration of the raw heat data yielded the observed heat Q as a function of SAMul concentration C, as shown in panel **A** of Figure S39.

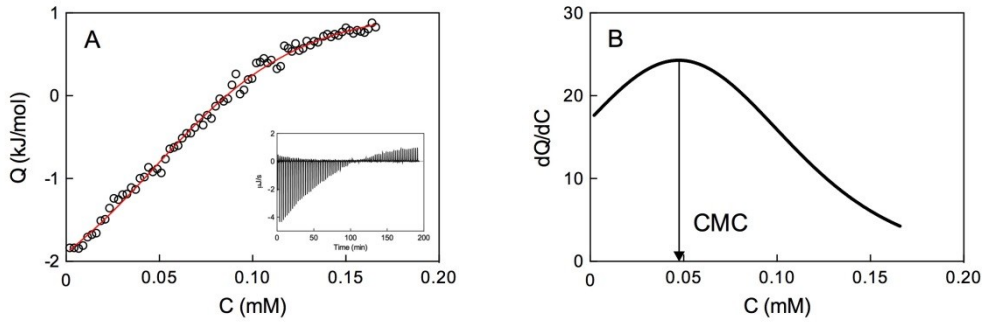


Fig. S39. (Left) ITC demicellization of $C_{16}$-D-Lys in Tris HCl 10mM/150 mM NaCl at 25°C. (A) Heat observed on each injection vs. final $C_{16}$-D-Lys concentration in the calorimetric cell. Symbols: experimental data; red line: Boltzmann fit ($R^2$ = 0.9946). Insert: Measured heat power vs. time elapsed during the titration. (B) The first derivative of the curve in A (in arbitrary units). The CMC is taken as the x-value at the maximum of dQ/dC curve (indicated by the arrow).

The CMC is defined as the midpoint of the Q vs. C curve in Figure S39 A. For a precise determination of the midpoint of the demicellization process, first Q vs C data are fitted to a suitable model and then the first derivative of the Q vs C fitting curve is calculated (Figure S39 B). The CMC corresponds to the maximum of the derivative

curve, as highlighted in Figure S39 B by the arrow.

Titration curves for the polyanion binding experiments are presented in the main paper In order to minimize the complexity of the ITC experiments, and given the purpose of validating the similar/differential behavior of the SAMul entities towards heparin and DNA, the concentration of the SAMul monomers employed was well above their corresponding CMC throughout the entire ITC titration. Figure S40 presents the thermodynamic data in graphical form (these data were tabulated in the main paper).

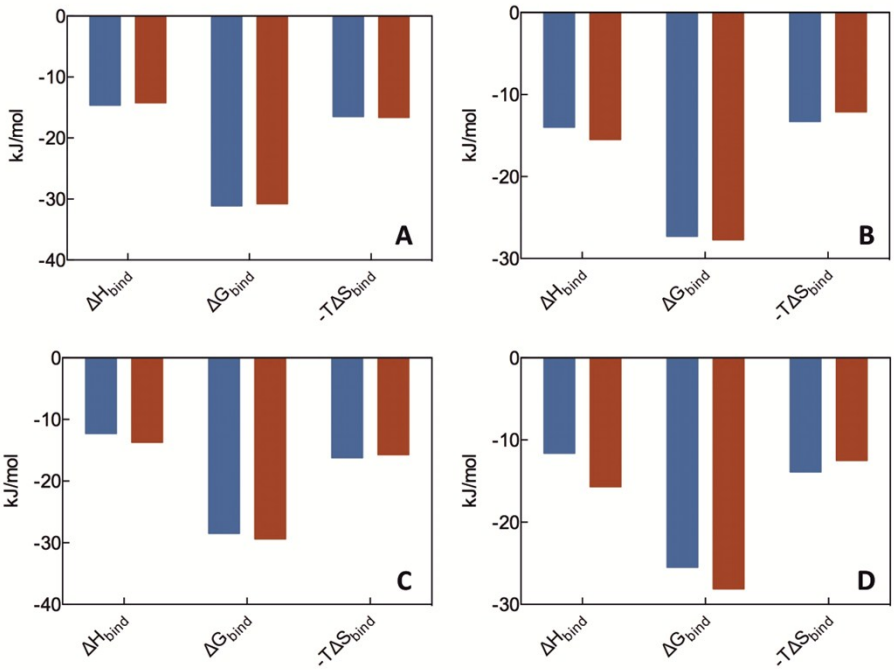


Fig. S40. ITC-determined thermodynamic parameters (binding enthalpy $\Delta H_{bind}$, binding free energy $\Delta G_{bind}$, and binding entropy $-T\Delta S_{bind}$) for $C_{16}$-L-Lys (blue) and $C_{16}$-D-Lys (red) in complex with heparin (A) and DNA (B), and for $C_{16}$-Gly-L-Lys (blue) and $C_{16}$-Gly-D-Lys (red) in complex with heparin (C) and DNA (D).

## 10. References


1. M. C. A. Stuart, J. C. van de Pas and J. B. F. N. Engberts, *J. Phys. Org. Chem.*, 2005, **18**, 929-934.
2. B. F. Cain, B. C. Baguley and W. A. Denny, *J. Med. Chem.*, 1978, **21**, 658-668.
3. H. Gershon, R. Ghirlando, S. B. Guttman and A. Minsky, *Biochemistry*, 1993, **32**,

7143-7151.

4. S. M. Bromfield and D. K. Smith, *J. Am. Chem. Soc.*, 2015, **137**, 10056-10059.